

Whole organism chemical screening identifies modulators of pancreatic β cell function

Hiroki Matsuda^{1*†}, Sri Teja Mullapudi¹, Yu Hsuan Carol Yang¹, Hideki Masaki², Daniel Hesselson^{3,4}, and Didier Y. R. Stainier^{1*}

Author affiliation:

1. Max Planck Institute for Heart and Lung Research, Department of Developmental Genetics, Bad Nauheim, Germany
2. Division of Stem Cell Therapy, The Institute of Medical Science, University of Tokyo, Tokyo, Japan
3. Garvan Institute of Medical Research, Diabetes and Metabolism Division, Sydney, Australia
4. St. Vincent's Clinical School, UNSW Sydney, Sydney, Australia

† Current affiliation: Department of Biomedical Sciences, College of Life Sciences, Ritsumeikan University, Kusatsu, Japan

*Corresponding authors

Hiroki Matsuda (hmatsud1@fc.ritsumei.ac.jp)

Department of Biomedical Sciences
Ritsumeikan University
Noji-higashi, Kusatsu, 525-8577, Japan
Phone: +81-77-599-4213

Didier Stainier (didier.stainier@mpi-bn.mpg.de)

Department of Developmental Genetics
Max Planck Institute for Heart and Lung Research
Ludwigstrasse 43, 61231 Bad Nauheim, Germany
Phone: +49 (0) 6032 705-1333
Fax: +49 (0) 6032 705-1304

Abstract

β cell loss and dysfunction play a critical role in the progression of type 1 and type 2 diabetes. Identifying new molecules and/or molecular pathways that improve β cell function and/or increase β cell mass should significantly contribute to the development of new therapies for diabetes. Using the zebrafish model, we screened 4640 small molecules to identify modulators of β cell function. This *in vivo* strategy identified 84 stimulators of *insulin* expression which simultaneously reduced glucose levels. The *insulin* promoter activation kinetics for 32 of these stimulators were consistent with a direct mode of action. A subset of *insulin* stimulators, including the antidiabetic drug Pioglitazone, induced the coordinated upregulation of gluconeogenic *pck1* expression, suggesting functional response to increased Insulin action in peripheral tissues. Notably, Kv1.3 inhibitors increased β cell mass in larval zebrafish and stimulated β cell function in adult zebrafish and in the STZ-induced hyperglycemic mouse model. In addition, our data indicate that cytoplasmic Kv1.3 regulates β cell function. Thus, using whole organism screening, we have identified new small molecule modulators of β cell function and glucose metabolism.

Introduction

Functional pancreatic endocrine cells, located in the islets of Langerhans, are crucial for blood glucose homeostasis. In response to changes in blood glucose levels, islets secrete hormones that act on peripheral tissues to normalize glucose levels. An example of this response is Insulin secretion by pancreatic β cells when blood glucose concentration increases after a meal. Insulin stimulates glucose uptake in peripheral tissues and the conversion of glucose to glycogen in the liver. Thus, optimal control of blood glucose levels depends on the precise control of Insulin production and secretion by the pancreatic β cells. Loss and dysfunction of β cells causes type 1 and type 2 diabetes, respectively. Therefore, identifying new molecules and/or molecular pathways that stimulate β cell function will contribute to the discovery of novel targets for future therapies for diabetes.

Phenotypic chemical screens using zebrafish (*Danio rerio*) have emerged as a powerful tool for rapid dissection of biological processes underlying complex traits (1). Over 50 screens have been reported spanning behavioral, cardiac, metabolic, and regenerative phenotypes (2), and these *in vivo* screening strategies have become an efficient platform to identify drug candidates for clinical repurposing (3). Zebrafish is particularly well suited to study pancreas development and physiology (4-8). Several groups, including ours, have previously performed zebrafish-based small molecule screens and reported novel molecules and signaling pathways that stimulated β cell differentiation, regeneration or proliferation (9-12). However, a screen targeting *in vivo* β cell function has not yet been reported.

Here, we performed a small molecule screen using the zebrafish model to identify *in vivo* modulators of β cell function and glucose metabolism. Using zebrafish larvae, we identified 84 *insulin* stimulators which reduced glucose levels, and 7 *insulin* repressors which increased glucose levels. Among the stimulators, we discovered the Kv1.3 blocker Psora4,

which also stimulated β cell function and peripheral insulin response and also reduced glucose levels in mouse. Additionally, our data indicate that cytoplasmic Kv1.3 modulates β cell function, revealing a new mechanism to modulate β cell function.

Research Design and Methods

Zebrafish lines

All zebrafish husbandry was performed under standard conditions in accordance with institutional and national ethical and animal welfare guidelines.

We used the following transgenic lines: *Tg(ins:Luc2;cryaa:mCherry)^{gi3}* (13), abbreviated *ins:Luc2*, *Tg(pck1:Luc2;cryaa:mCherry)^{s952}* (14), abbreviated *pck1:Luc2*, *Tg(ins:H2BGFP;ins:dsRED)^{s960}* (15), abbreviated *ins:H2BGFP*, *Tg(P0-pax6b:eGFP)^{ulg515}* (16), abbreviated *pax6b:eGFP*, *TgBAC(neurod1:eGFP)ⁿ¹¹* (17), abbreviated *neurod1:eGFP*, and *Tg(-2.6mnx1:GFP)^{ml59}* (18), abbreviated *mnx1:eGFP*.

Luciferase assay and small molecule screening.

The *ins:Luc2* zebrafish line was incrossed, the progeny raised and screened for homozygous transgenic animals, which were then outcrossed to AB wild-type zebrafish to collect large numbers of heterozygous transgenic animals for experiments. Healthy larvae (4 dpf) were selected and washed with egg water before distributing three animals per well in 200 μ l 10mM Hepes buffered egg water in 96-well plates. Drugs were diluted from a 1 mM stock solution in DMSO to a treatment concentration of 10 μ M in 1% DMSO. After 48 h of treatment, the samples were incubated in Steady Glo (Promega) as described previously (14). Bioluminescence signal was analyzed by FLUOstar Omega (BMG LABTECH).

For the small molecule screen, three 4 dpf larvae were tested in duplicate for every compound. Differential modulation of *insulin* promoter activity was determined by normalizing to the average of the DMSO control in each plate. An average of 2.5 fold upregulation or 0.5 fold downregulation was assigned as the threshold for calling hits, which were further tested in validation experiments and glucose measurements.

Glucose measurements and treatments

After drug treatment, 15 larvae per group were homogenized and free glucose levels were determined by using a glucose assay kit (BioVision) as described previously (14). Blood glucose measurements in adult zebrafish were performed as described previously (13).

qRT-PCR

Total RNA from control and drug-treated larvae was extracted by RNeasy Mini Kit (Qiagen). Reverse transcription/polymerase chain reaction (RT-PCR) was performed by using SuperScript III First-Strand Synthesis System (Invitrogen) according to manufacturer's instructions with 500 ng total RNA as template.

qRT-PCR was performed with 2xDynamo Color Flash SYBR Green master mix (Thermo Scientific) and gene expression levels were quantified on a CFX Connect Real-time System (Bio Rad) with gene-specific primers (Supplementary Table 5). Each sample was normalized to a housekeeping gene (*actb*).

Plasma Insulin detection

Plasma Insulin detection was performed as described previously (13).

Fluorescence imaging and immunostaining

Fluorescence images were acquired with an LSM 700 laser scanning confocal microscope (Carl Zeiss), and fluorescence intensity of each transgenic line was calculated using the ZEN software. Cell numbers were counted manually for experiments using the *ins:H2BGFP* transgenic line.

Immunostaining was performed as described previously (19). The following primary antibodies were utilized at the indicated dilutions in 1% FBS in PBS-containing 0.1% Triton X-100 (PBTx): Guinea pig anti-Insulin (Abcam) at 1:100, and rabbit anti-Kv1.3 (Anemone Labs) at 1:100 (20, 21). AlexaFluor-conjugated secondary antibodies (Invitrogen) were used at 1:500-1:1000 dilution with 1% FBS in PBTx.

Insulin secretion from mouse islets

Pancreatic islets were isolated from 16 to 20-week-old C57BL/6J mice following LiberaseTL (Roche) infusion via the common bile duct to disrupt the pancreatic exocrine tissue and filtration to recover intact islets. Islets were hand-picked and cultured overnight in RPMI1640 supplemented with 10% FBS, 100 units/ml penicillin, and 100 μ g/ml streptomycin. Islets were treated with 10 μ M of the hit compounds for 24 h in RPMI1640 containing 0.2% BSA, 100 units/ml penicillin, and 100 μ g/ml streptomycin. Glucose stimulated Insulin secretion was conducted in KRB buffer containing 4.6 mM KCl, 2.5 mM CaCl₂, 1.2 mM MgSO₄, 1.2 mM KH₂PO₄, 17.7 mM NaHCO₃, 10 mM HEPES, 117 mM NaCl and 0.2% BSA. 10 size-matched islets were pre-incubated for 1 h in KRB containing 3 mM glucose prior to collection of the supernatant from incubations with fresh KRB containing 3 or 15 mM glucose. Insulin secretion was assessed with a mouse Insulin ELISA kit (Alpco) following manufacturer's protocol.

Mouse experiments

Hyperglycemia was induced in 8-week-old C57BL/6N male mice by intraperitoneal injection of 150 mg/kg STZ (22). Mice with non-fasting blood glucose levels over 350 mg/dl one week after STZ administration were used. Psora-4 was dissolved in peanut oil at 10 mg/ml with stirring at 70 °C, and intraperitoneally injected to diabetic mice at 40 mg/kg. 100 μ l peanut oil was injected as a control. After 6 hours of fasting, blood glucose levels were measured by MS-GT102 (Terumo) from peripheral blood obtained from the tail vein every 24 hours starting at one day before the injection. Glucose tolerance test was performed at 5 days after Psora4 injection. Blood glucose levels were measured at 0, 15, 30, 60, 90 and 120 min after intraperitoneal injection of 2 g/kg glucose after 6 hours of fasting. Insulin tolerance test was performed at 5 days after Psora4 injection. Blood glucose levels were measured after intraperitoneal injection of 0.5 U/kg Humalin R (Eli Lilly) after 6 hours of fasting. All mouse experiments were approved by the Institutional Animal Care and Use Committee, and performed in accordance with the guidelines of the University of Tokyo.

Results

A whole-organism screen for modulators of β cell function

To enable high throughput small molecule screening for modulators of β cell function, we first optimized the quantification of *insulin* expression using an *in vivo* luciferase transgenic reporter (*ins:Luc2*) (13). We identified the optimal treatment window for screening using known modulators of β cell differentiation (DAPT) (23), proliferation (RA, glucocorticoids, trazodone, prednisolone) (11) and maturation (T3) (13) (Fig. 1A and B, and Supplementary Figure 1). We determined that treatments from 4-6 days post-fertilization (dpf) generated the greatest dynamic range in the assay. Therefore, we performed a primary screen of 4640 small molecules from 4-6 dpf at a fixed concentration of 10 μ M. We identified 229 small molecules that enhanced *insulin* reporter activity by at least 2.5 fold and

31 small molecules that repressed *insulin* reporter activity to less than half of the DMSO control samples (Fig. 1C).

Next, we applied a functional filter to identify compounds that were likely to modulate endogenous *insulin* expression. In the absence of compensatory responses, we predicted that *insulin* expression and glucose levels would be inversely correlated. Zebrafish larvae were treated with the hit compounds from 4 to 6 dpf and free glucose levels were analyzed. In these experiments, 84 of the 229 *insulin* stimulators showed over 20 % glucose reduction and 7 of the 31 *insulin* repressors showed over 20 % glucose elevation (Fig. 1D). Thus, these 91 compounds (1.96% of the library), affecting both *insulin* reporter expression and glucose metabolism, were selected for subsequent analyses.

The 48 hour small molecule treatments used in the primary screen may have had direct effects on *insulin* transcription and/or indirect effects on β cell function, as a consequence of other physiological changes in metabolism. In order to identify small molecules that were most likely to directly modulate *insulin* expression, shorter drug treatment windows were tested using the *ins:Luc2* line. After 12 h drug treatments, 32 of the 84 stimulators from the primary screen enhanced the activity of the *insulin* expression reporter (12 h *insulin* stimulators) (Fig. 1E, Table 1 and Supplementary Table 1). An additional 14 compounds required 24 h of exposure to enhance *insulin* expression reporter activity (24 h *insulin* stimulators) (Fig. 1E and Supplementary Table 2). The remaining 38 *insulin* stimulators were only active under the original screening conditions (48 h *insulin* stimulators) (Fig. 1E and Supplementary Table 3), suggesting that this class indirectly induced *insulin* reporter expression. Surprisingly, 2 of the 7 *insulin* repressors from the primary screen stimulated *insulin* promoter activity in 12 or 24 h assays, suggesting that they

induce a compensatory response at 48 h. The 5 remaining *insulin* repressors required 48 h to repress *ins:Luc2* in the assay (Fig. 1E and Supplementary Table 4).

The glucoregulatory effects of the *insulin* reporter modulators could be due to effects on gluconeogenesis itself. To investigate this possibility, we used a validated *pck1:Luc2* reporter (14) to quantify the effects of the primary hits on the expression of a key, transcriptionally regulated, gluconeogenic enzyme. We classified small molecules that increased reporter activity by more than 3.5 fold as “strong *pck1* inducers”, compounds that increased reporter activity from 1 to 3.5 fold as “weak *pck1* inducers”, and drugs that led to reporter activity to less than 1 fold as “*pck1* repressors” (Fig. 1F).

Characterization of 2,4-DB, GNTI, Psora4, SR-2640 and Karanjin effect in larval zebrafish

We prioritized the 12 h *insulin* stimulators for additional analyses because they were most likely to act directly on β cells. Furthermore, we filtered the 12 h *insulin* stimulators to identify those that lowered glucose levels despite elevated *pck1* expression, since enhanced gluconeogenesis could represent a homeostatic response to increased Insulin action. Based on these criteria, we selected 13/32 of the 12 h *insulin* stimulators for further investigation (Fig. 1F and Table 1). Compensatory gluconeogenesis could reflect increased β cell function and/or Insulin sensitivity in target tissues. Interestingly, the 13 compounds included Pioglitazone, a frequently prescribed antidiabetic drug of the thiazolidinedione family, which stimulates both β cell function and Insulin sensitivity in peripheral tissues (24, 25). To identify novel β cell stimulators, we selected six compounds among the remaining twelve that had not been previously characterized in detail: 2,4-DB (auxin), GNTI (OPRK antagonist), Psora-4 (Kv1.3 blocker), 2',4'-D-4-M (chalcone), SR-2640 (LTD4/LTE4) and Karanjin (flavonoid). Since the primary screen was performed at a fixed dose of 10 μ M, we performed

dose-response assays (0-100 μ M) to determine the most effective concentration for each compound. Using acute 12 h treatments, we determined the concentration of each compound that elicited maximal induction of the *ins:Luc2* reporter (Supplementary Figure 2), which was then used in subsequent experiments. For compounds that exhibited toxicity at higher doses, we determined dose-dependent survival (Supplementary Figure 3) and excluded 2',4'-D-4-M from further analysis due to complete lethality at 20 μ M (double the primary screening dose).

The effects of the remaining five compounds (2,4-DB, GNTI, Psora-4, SR-2640 and Karanjin; Fig. 2A) on the expression level of endogenous *insulin* were quantified in wild-type zebrafish (Supplementary Figure 4A and B). All of the compounds stimulated endogenous *insulin* expression after acute (12 hour) as well as 48 hour treatments (Supplementary Figure 4A and B), further validating the primary screen. To determine whether the drug treatments impacted β cell mass as a result of increased proliferation or differentiation, we treated *ins:H2BGFP* reporter fish, which express a stabilized nuclear-localized GFP that facilitates cell number quantification, starting at 4 dpf (Fig. 2B-G). As expected, based on the effects on endogenous *insulin* expression levels, *ins:H2BGFP* intensity was increased by all compounds by 6 dpf (Fig. 2E-G). Quantification of β cell numbers revealed a small but significant increase in β cell mass by 7 dpf with Psora4, SR-2640 and Karanjin treatments and no effect with 2,4-DB or GNTI treatments (Fig. 2E-G), further suggesting that Psora4, SR-2640 and Karanjin have effects on β cell differentiation and/or proliferation.

Effects of 2,4-DB, GNTI, Psora4, SR-2640 and Karanjin on the expression of endocrine markers

To understand how these compounds regulate *insulin* expression, we investigated the effects of these compounds on upstream endocrine transcription factor genes. We used

transcriptional eGFP reporters for *pax6b*, *neurod* and *mnx1*, which encode known regulators of *insulin* expression and endocrine differentiation, and then analyzed eGFP expression in the principal islet (Fig.3 and supplementary Figure 6). Interestingly, all compounds enhanced *mnx1*:eGFP expression by 2 days of treatment (Fig.3F and G) without altering *mnx1*:eGFP expression after 24 hours of treatment (Supplementary Figure 6C). These data suggest that mechanisms used for enhancement of *insulin* expression at 12 hours of treatment are different from those used for maintenance of *insulin* expression at the later time points (24 or 48 hours). Furthermore, qPCR analysis revealed that SR2640 and Psora4 enhanced *pdx1* expression at 2 days of treatment, but not at 12 hours of treatment (Supplementary Figure 4A and B). Altogether, these data suggest that five compounds (2,4-DB, GNTI, Psora4, SR-2640 and Karanjin) affect the expression of developmental endocrine regulators, as well as that of *insulin*.

2-4DB, GNTI, Psora4, SR-2640 and Karanjin stimulate Insulin secretion in vivo

Adults possess glucoregulatory mechanisms that are not present during development. To determine whether our prioritized *insulin* activators induced hypoglycemia in adult zebrafish, we injected adult animals with each compound daily and measured blood glucose levels after the third injection (Fig. 4A). Encouragingly, none of the compounds caused hypoglycemia under basal conditions (Fig. 4B); and in an intraperitoneal (IP) glucose tolerance test, four of the compounds (GNTI, Psora4, SR2640 and Karanjin) improved blood glucose clearance (Fig. 4B). Furthermore, and consistent with the effects on larval *insulin* expression, all of the compounds increased blood Insulin levels after glucose challenge (Fig. 4C and D), indicating that the drug treatments potentiated Insulin secretion from β cells.

Kv1.3 inhibitors stimulate Insulin secretion in isolated mouse islets

To determine whether the *insulin* stimulating effects were conserved in a mammalian model, we measured Glucose Stimulated Insulin Secretion (GSIS) from isolated mouse islets that were treated for 24 h with each compound (Fig. 5A). Only Psora4 potentiated GSIS in mouse islets (Fig. 5A). To establish whether the effects of Psora4 on *insulin* expression and β cell function are mediated by on-target Kv1.3 inhibition, we tested two other Kv1.3 inhibitors, PAP-1 and clafozamine (supplementary Figure 7). Both PAP-1 and clafozamine stimulated *insulin* expression upon 12 hours of treatment (supplementary Figure 7A and B), although both PAP-1 and clafozamine exhibited higher toxicity than Psora4 (supplementary Figure 7A and supplementary Figure 8A-C). Furthermore, both PAP-1 and clafozamine lowered blood glucose levels (supplementary Figure 7F), and enhanced blood Insulin secretion (supplementary Figure 7G and H) in adult zebrafish. Additionally PAP-1 increased β cell numbers and *ins:eGFP* expression in larval zebrafish (supplementary Figure 7C and D). We conclude that the metabolic effects of Psora4 are likely through on-target Kv1.3 inhibition. Next, to confirm that the effects of Kv1.3 inhibition were glucose-dependent, we sequentially incubated Psora4, PAP-1 or vehicle-treated mouse islets in low (3 mM), high (15 mM), and low (3 mM) glucose media. Psora4 and PAP-1 treated islets exhibited enhanced glucose-dependent Insulin secretion that returned to baseline (Fig. 5B and C). Importantly, Insulin secretion returned to basal levels when the islets were re-exposed to 3 mM glucose, suggesting that beta cell re-polarization was not affected by Kv1.3 inhibition. Psora4 and PAP-1 had modest effects on *Ins1* and *Ins2* expression (supplementary Figure 9), suggesting that in mouse these compounds stimulate Insulin secretion mostly through a post-transcriptional mechanism.

Psora4 reduces blood glucose levels in hyperglycemic mice by enhancing Insulin secretion

We administered Psora4 to the streptozotocin (STZ)-induced mouse diabetes model to determine whether Psora4 can improve glucose metabolism *in vivo*. Following confirmation of STZ-induced hyperglycemia (>350 mg/dl), Psora4 was delivered by IP injection, and blood glucose levels were monitored daily after 6 h of fasting. Compared with vehicle-injected mice, blood glucose levels in Psora4-injected mice were markedly reduced by 1 day after the first Psora4 injection and remained lower with every other day treatments (Fig. 6A, B). A glucose tolerance test at 5 days after the first Psora4 injection showed improved glucose tolerance in the Psora4-treated animals (Fig. 6C, D), accompanied by increased Insulin secretion (Fig. 6E). Finally, we performed an Insulin challenge after 7 days of Psora4 treatment. Blood glucose levels were modestly, yet significantly, lower in Psora4-treated animals (Fig. 6F, G). Together, our data indicate that Psora4 exhibits conserved effects on glucose metabolism *in vivo*, mainly by increasing Insulin secretion.

Kv1.3 appears to be localized in the cytoplasm of pancreatic β cells.

There are no previous reports on Kv1.3 expression in pancreatic β cells, although Kv1.3 has been detected in islets by RT-PCR (26). Therefore, we investigated Kv1.3 expression mouse (Fig. 7A) and zebrafish (Fig. 7B) islets using an antibody, which recognized a C-terminal regions of mammalian Kv 1.3 (supplementary Figure 10) and has been used on rat brain sections (21) as well as on western blots of mouse samples (20). Surprisingly, Kv1.3 immunostaining was mostly localized in the cytoplasm, but not at the cell membrane, of mouse pancreatic β cells (Fig. 7A). In these cells, Kv1.3 immunostaining was observed in a subset of insulin granules (Fig. 7A). Using this antibody, we also observed immunostaining in the cytoplasm and nucleus of zebrafish β cells at 5 dpf (Fig. 7B). Altogether, these results suggest a putative novel role for cytoplasmic Kv1.3 in glucose stimulated Insulin secretion.

Discussion

In this study, we screened 4640 small molecules using zebrafish and identified 91 compounds which affected *insulin* expression and glucose homeostasis. We found that a voltage-gated potassium (Kv) channel 1.3 inhibitor, Psora4, stimulated Insulin secretion and reduced blood glucose levels in zebrafish and mice. Furthermore, our results suggest that Psora4 might act as a direct regulator of *insulin* expression, because Psora4 induced expression of *insulin* within 12 hours without upregulating other endocrine differentiation genes. Although Kv1.3 expression was previously detected in rat islets (26), it has been unclear how Kv1.3 functions in pancreatic β cells. On the other hand, other members of the Kv channel subfamily are expressed in pancreatic β cells and their functions in β cells has been reported (26-33). During glucose stimulated Insulin secretion, high glucose causes the closure of ATP-sensitive K^+ channels (K_{ATP} channels), thereby causing β cell depolarization which leads to the activation of voltage dependent Ca^{2+} channels, and then stimulation of Insulin secretion. It has been proposed that Kv channels control membrane repolarization and thereby suppress prolonged Insulin secretion (27). This model assumes that Kv channels are localized to the plasma membrane. However, Kv 1.3 appears to be localized mostly to the cytoplasm of zebrafish and mouse β cells, and to the best of our knowledge, it has not been clearly determined where other Kv channels are localized in pancreatic β cells. However, additional reagents, including Kv 1.3 null mutant and GFP tagged Kv1.3 will be required to determine the precise localization of Kv 1.3, and related channels, to further explore this model. It is also unclear how Kv channels are trafficked, how they function, and whether Kv channels have cytoplasmic roles in other tissues. A deeper understanding of cytoplasmic Kv channel regulation may reveal new regulatory mechanisms for Insulin secretion in pancreatic β cells. Kv1.3 blockers have been shown to improve peripheral

insulin sensitivity (34, 35), enhance metabolic rate and weight loss (36), and decrease the incidence of autoimmune diabetes in a type 1 diabetes rat model by resetting T cell memory (37). We propose that the reduced blood glucose levels in STZ treated mice injected with Psora4 due to the combined effects of Kv1.3 inhibition on Insulin production and peripheral Insulin sensitivity. Therefore, the Kv family, including Kv1.3, are promising targets for anti-diabetic drug discovery and Psora4 is an interesting candidate to investigate a new class of anti-diabetic drug.

Our investigation of 4 additional compounds - 2,4DB, GNTI, SR2640 and Karanjin- showed that they stimulated *insulin* expression and reduced glucose levels in larval zebrafish and increased Insulin secretion in adult zebrafish. Furthermore, GNTI, SR2640 and Karanjin reduced blood glucose levels in adult zebrafish, and SR2640 and Karanjin increased β cell mass in larval zebrafish. However, none of these compounds could stimulate Insulin secretion in mouse islets. These results suggest the possibility that these compounds do not act on β cells directly or that the mechanism of action for these drugs differs between species. However, it is also possible that differences in results arise from the *in vitro* and *in vivo* nature of the experiments. For example, SR2640 and GNTI inhibit the function of receptors by competing with their ligands. Therefore, these compounds cannot inhibit the functions of these receptors under conditions without ligands, as is possibly the case with *in vitro* mouse islet culture experiments. Furthermore, it has been reported that the action of thyroid hormone is different between isolated islets and *in vivo* islets (38). Thus, isolated islets might not perfectly mimic *in vivo* islet behavior. In addition, metabolites of these compounds, but not compounds themselves, might be the active agents. As another example, it has been reported that Karanjin can reduce blood glucose levels in STZ-treated and *db/db* mice (39), although it is unclear whether it acts directly on pancreatic β cells. Thus, it will be interesting

to investigate how these drugs affect mammalian β cells *in vivo* and consequently organismal glucose metabolism.

In our study, many interesting compounds were identified. For example, levothyroxine (thyroid hormone receptor agonist), Harmine (DYRK1A inhibitor), and Bay K8644 (calcium channel activator), three known stimulators of *Mafa* expression and/or β cell maturation (38, 40-43), turned up in the list of 84 *insulin* stimulators. These 84 compounds are likely to include new drugs that stimulate β cell maturation as well as β cell function. In addition, 4/84 compounds caused a decrease in *pck1* activity. These compounds hold high potential in anti-diabetes therapy, because they not only stimulate Insulin production, but also reduce gluconeogenesis. In addition, we reported that 6 other compounds reduced glucose levels and that 43 compounds, including 7 *insulin* repressors, elevated glucose levels (Fig. 1D). Investigating downstream mechanisms of these molecules in detail should provide new insights into glucose metabolism. Furthermore, another 127 compounds from the screen modulated *insulin* promoter activity without changing organismal glucose levels. Therefore, it will be interesting to investigate the effects of these compounds on β cell differentiation and proliferation, as they could aid *in vitro* differentiation protocols. Thus, our screen has identified several classes of drugs of interest to the fields of β cell biology, glucose homeostasis, and anti-diabetic therapies.

Acknowledgement

This work was supported in part by funds from the Max Planck Society and the EU (HumEn) to D.Y.R.S. H.M. and D.Y.R.S. conceived the project. H.M., S.T.M., Y.H.C.Y., H.M., D. H. and D.Y.R.S. contributed to discussion of data and to editing and writing the manuscript. H.M., S.T.M., Y.H.C.Y. and H.M. generated data. H.M. and D.Y.R.S. are the guarantors of this work and, as such, had full access to all of the data in the study and take

responsibility for the data and the accuracy of the data analysis. We have no conflicts of interest to declare.

We thank Viola Graef for critical reading of the manuscript, Sabine Fischer for help with the animal protocols, all members of the Stainier lab for helpful discussion and the fish facility staff for fish care.

References

1. Gut P, Reischauer S, Stainier DYR, Arnaout R. Little fish, big data: Zebrafish as a model for cardiovascular and metabolic disease. *Physiol Rev.* 2017;97:889-938.
2. Rennekamp AJ, Peterson RT. 15 years of zebrafish chemical screening. *Curr Opin Chem Biol.* 2014; 58–70.
3. Griffin A, Hamling KR, Knupp K, Hong S, Lee LP, Baraban SC. Clemizole and modulators of serotonin signaling suppress seizures in Dravet syndrome. *Brain.* 2017; 1093
4. Field HA, Dong PD, Beis D, Stainier DY. Formation of the digestive system in zebrafish. II. Pancreas morphogenesis. *Dev Biol* 2003; 261:197-208.
5. Kinkel MD, Prince VE. On the diabetic menu: zebrafish as a model for pancreas development and function. *Bioessays* 2009; 31:139-152.
6. Tiso N, Moro E, Argenton F. Zebrafish pancreas development. *Mol Cell Endocrinol* 2009; 312:24-30.
7. Kimmel RA, Meyer, D. Zebrafish pancreas as a model for development and disease. *Methods in Cell Biol.* 2016; 134:431-461
8. Matsuda H. Zebrafish as a model for studying functional pancreatic β cells development and regeneration. *Dev. Growth. Differ.* 2018. in press.

9. Andersson O, Adams BA, Yoo D, Ellis GC, Gut P, Anderson RM, German MS, Stainier DY. Adenosine signaling promotes regeneration of pancreatic β Cells in Vivo. *Cell Metab.* 2012;6:885-894
10. Rovira M, Huang W, Yusuff S, Shim JS, Ferrante AA, Liu JO, Parsons MJ. Chemical screen identifies FDA-approved drugs and target pathways that induce precocious pancreatic endocrine differentiation. *Proc Natl Acad Sci U S A.* 2011;108:19264-19269
11. Tsuji N, Ninov N, Delawary M, Osman S, Roh AS, Gut P, Stainier DY. Whole organism high content screening identifies stimulators of pancreatic beta-cell proliferation. *PLoS One.* 2014;12:e104112.
12. Wang G, Rajpurohit SK, Delaspre F, Walker SL, White DT, Ceasrine A, Kuruvilla R, Li RJ, Shim JS, Liu JO, Parsons MJ, Mumm JS. First quantitative high-throughput screen in zebrafish identifies novel pathways for increasing pancreatic β -cell mass. *Elife.* 2015; eLife.08261.
13. Matsuda H, Mullapudi ST, Zhang Y, Hesselson D, and Stainier DYR. Thyroid hormone coordinates pancreatic islet function during the zebrafish larval to juvenile transition to maintain glucose homeostasis. *Diabetes.* 2017; 66(10): 2623-2635
14. Gut P, Baeza-Raja B, Andersson O, Hasenkamp L, Hsiao J, Hesselson D, Akassoglou K, Verdin E, Hirschey MD, Stainier DY. Whole-organism screening for gluconeogenesis identifies activators of fasting metabolism. *Nat Chem Biol.* 2013;9: 97–104.
15. Curado S, Anderson RM, Jungblut B, Mumm J, Schroeter E, Stainier DY. Conditional targeted cell ablation in zebrafish: A new tool for regeneration studies. *Dev Dyn.* 2007;236:1025-1035.

16. Delporte FM, Pasque V, Devos N, Manfroid I, Voz ML, Motte P, Biemar F, Martial JA, Peers B. Expression of zebrafish *pax6b* in pancreas is regulated by two enhancers containing highly conserved cis-elements bound by PDX1, PBX and PREP factors. *BMC Dev Biol* 2008;8:53.
17. Obholzer N, Wolfson S, Trapani JG, Mo W, Nechiporuk A, Busch-Nentwich E, Seiler C, Sidi S, Söllner C, Duncan RN, Boehland A, Nicolson T. Vesicular glutamate transporter 3 is required for synaptic transmission in zebrafish hair cells. *J Neurosci* 2008;28: 2110-2118.
18. Arkhipova V, Wendik B, Devos N, Ek O, Peers B, Meyer D. Characterization and regulation of the *hb9/mnx1* beta-cell progenitor specific enhancer in zebrafish. *Dev Biol* 2012;365: 290–302.
19. Matsuda H, Parsons MJ, Leach SD. Aldh1-expressing endocrine progenitor cells regulate secondary islet formation in larval zebrafish pancreas. *PLoS One* 2013;8:e74350.
20. Moreno C, Prieto P, Macías Á, Pimentel-Santillana M, de la Cruz A, Través PG, Boscá L, Valenzuela C. Modulation of voltage-dependent and inward rectifier potassium channels by 15-epi-lipoxin-A4 in activated murine macrophages: implications in innate immunity. *J Immunol.* 2013;191:6136-6146.
21. Wolff M, Czorlich P, Nagaraj C, Schnöbel-Eehalt R, Li Y, Kwapiszewska G, Olschewski H, Heschl S, Olschewski A. Amitriptyline and carbamazepine utilize voltage-gated ion channel suppression to impair excitability of sensory dorsal horn neurons in thin tissue slice: An in vitro study. *Neurosci Res.* 2016;109:16-27.
22. Yamaguchi T, Sato H, Kato-Itoh M, Goto T, Hara H, Sanbo M, Mizuno N, Kobayashi T, Yanagida A, Umino A, Ota Y, Hamanaka S, Masaki H, Rashid ST, Hirabayashi M, Nakauchi H. Interspecies organogenesis generates autologous functional islets.

- Nature. 2017; 542:191-196.
23. Parsons MJ, Pisharath H, Yusuff S, Moore JC, Siekmann AF, Lawson N, Leach SD. Notch-responsive cells initiate the secondary transition in larval zebrafish pancreas. *Mech Dev.* 2009;126: 898-912
24. Kemnitz JW, Elson DF, Roecker EB, Baum ST, Bergman RN, Meglasson MD. Pioglitazone Increases Insulin Sensitivity, Reduces Blood Glucose, Insulin, and Lipid Levels, and Lowers Blood Pressure, in Obese, Insulin-Resistant Rhesus Monkeys. *Diabetes.* 1994; 43: 204-211
25. Gastaldelli A, Ferrannini E, Miyazaki Y, Matsuda M, Mari A, DeFronzo RA. Thiazolidinediones improve β -cell function in type 2 diabetic patients. *Am J Physiol Endocrinol Metab.* 2007 ;292: E871-883.
26. MacDonald PE and Wheeler MB. Voltage-dependent K^+ channels in pancreatic beta cells: Role, regulation and potential as therapeutic targets. *Diabetologia.* 2003; 46:1046–1062
27. MacDonald PE, Joseph JW, Rorsman P. Glucose-sensing mechanisms in pancreatic b-cells. *Phil Trans R Soc B* 2005;360: 2211–2225
28. MacDonald PE, Ha XF, Wang J, Smukler SR, Sun AM, Gaisano HY, Salapatek AMF, Backx PH, Wheeler MB. Members of the Kv1 and Kv2 Voltage-Dependent K Channel Families Regulate Insulin Secretion. *Mol Endocrinol.* 2001; 15:1423–1435
29. Ma Z, Lavebratt C, Almgren M, Portwood N, Forsberg LE, Branstrom R, Berglund E, Falkmer S, Sundler F, Wierup N, Bjorklund A. Evidence for Presence and Functional Effects of Kv1.1 Channels in β Cells: General Survey and Results from mceph/mceph Mice. *PLoS ONE.* 2011; 6(4): e18213
30. Finol-Urdaneta RK, Remedi MS, Raasch W, Becker S, Clark RB, Struver N, Pavlov E, Nichols CG, French RJ, Terlau H. Block of $K_v1.7$ potassium currents increases

- glucose-stimulated insulin secretion. *EMBO Mol Med.* 2012; 4: 424–434
31. Kim SJ, Widenmaier SB, Choi WS, Nian C, Ao Z, Warnock G, McIntosh CH. Pancreatic β -cell prosurvival effects of the incretin hormones involve post-translational modification of Kv2.1 delayed rectifier channels. *Cell Death Differ.* 2012; 19: 333–344.
 32. Kim SJ, Ao Z, Warnock G, Mcintosh CH. Incretin-stimulated interaction between β -cell Kv1.5 and Kv β 2 channel proteins involves acetylation/deacetylation by CBP/SirT1. *Biochem. J.* 2013; 451: 227–234
 33. Zhou TT, Quan LL, Chen LP, Du T, Sun KX, Zhang JC, Yu L, Li Y, Wan P, Chen LL, Jiang BH, Hu LH, Chen J, Shen X. SP6616 as a new Kv2.1 channel inhibitor efficiently promotes β -cell survival involving both PKC/Erk1/2 and CaM/PI3K/Akt signaling pathways. *Cell Death and Disease.* 2016; 7: e2216
 34. Xu J, Wang P, Li Y, Li G, Kaczmarek LK, Wu Y, Koni PA, Flavell RA, Desir GV. The voltage-gated potassium channel Kv1.3 regulates peripheral insulin sensitivity. *Proc Natl Acad Sci U S A.* 2004; 101:3112-3117.
 35. Tschritter O, Machicao F, Stefan N, Schafer S, Weigert C, Staiger H, Spieth C, Haring HU, Fritsche A. A new variant in the human Kv1.3 gene is associated with low insulin sensitivity and impaired glucose tolerance. *J Clin Endocrinol Metab.* 2006;91: 654-658.
 36. Xu J, Koni PA, Wang P, Li G, Kaczmarek L, Wu Y, Li Y, Flavell RA, Desir GV. The voltage-gated potassium channel Kv1.3 regulates energy homeostasis and body weight. *Hum Mol Genet.* 2003;12:551-559.
 37. Beeton C, Wulff H, Standifer NE, Azam P, Mullen KM, Pennington MW, Kolski-Andreaco A, Wei E, Grino A, Counts DR, Wang PH, LeeHealey CJ, S Andrews B, Sankaranarayanan A, Homerick D, Roeck WW, Tehranzadeh J, Stanhope KL, Zimin

- P, Havel PJ, Griffey S, Knaus HG, Nepom GT, Gutman GA, Calabresi PA, Chandy KG. Kv1.3 channels are a therapeutic target for T cell-mediated autoimmune diseases. *Proc Natl Acad Sci U S A*. 2006;103:17414-17419.
38. Aguayo-Mazzucato C, Zavacki AM, Marinelarena A, Hollister-Lock J, El Khattabi I, Marsili A, Weir GC, Sharma A, Larsen PR, Bonner-Weir S. Thyroid hormone promotes postnatal rat pancreatic β -cell development and glucose-responsive insulin secretion through MAFA. *Diabetes* 2013;62:1569-1580.
39. Tamrakar AK, Yadav PP, Tiwari P, Maurya R, Srivastava AK, Srivastava. Identification of pongamol and karanjin as lead compounds with antihyperglycemic activity from *Pongamia pinnata* fruits. *J Ethnopharmacol*. 2008;118:435-439
40. Pagliuca FW, Millman JR, Gürtler M, Segel M, Van Dervort A, Ryu JH, Peterson QP, Greiner D, Melton DA. Generation of functional human pancreatic β cells in vitro. *Cell* 2014;159(2):428-439.
41. Rezanian A, Bruin JE, Arora P, Rubin A, Batushansky I, Asadi A, O'Dwyer S, Quiskamp N, Mojibian M, Albrecht T, Yang YH, Johnson JD, Kieffer TJ. Reversal of diabetes with insulin-producing cells derived in vitro from human pluripotent stem cells. *Nat Biotechnol* 2014;32:1121-1133.
42. Wang P, Alvarez-Perez JC, Felsenfeld DP, Liu H, Sivendran S, Bender A, Kumar A, Sanchez R, Scott DK, Garcia-Ocaña A, Stewart AF. A high-throughput chemical screen reveals that harmine-mediated inhibition of DYRK1A increases human pancreatic beta cell replication. *Nat Med*. 2015;21:383-388.
43. Zhu S, Russ HA, Wang X, Zhang M, Ma T, XucT, Tang S, Hebrok M, Ding S. Human pancreatic beta-like cells converted from fibroblasts. *Nat Commun*. 2016;7:10080.
44. Hesselton D, Anderson RM, Beinat M, Stainier DY. Distinct populations of quiescent

and proliferative pancreatic beta-cell identified H₂O₂ mediated labeling. Proc Natl Acad Sci U S A. 2009;106:14896-14901.

45. Ye L, Robertson MA, Hesselton D, Stainier DY, Anderson RM. Glucagon is essential for alpha cell transdifferentiation and beta cell neogenesis. Development. 2015;142:1407-1417.

Figure legends

Fig. 1. Identifying modulators of *insulin* expression. (A and B) Assessment of *insulin* promoter activity using a *Tg(ins:Luc2)* zebrafish line. To determine the optimal treatment window, effects of known stimulators of *insulin* expression were tested across various developmental windows and treatment from 4 to 6 dpf was determined to be the most effective. (C) Small molecule screen for modulators of *insulin* expression. 4640 small molecules were screened at 10 μ M. Based on luminescence measurements, molecules which enhanced luciferase activity were termed *insulin* stimulators and molecules which reduced luciferase activity to under 0.5 fold were termed *insulin* repressors. 229 *insulin* stimulators and 31 repressors were identified. Blue dots indicate the values of the negative control samples (DMSO). Orange dots indicate the values of the positive control samples (T3 and trazodone). (D) Comparison between *insulin* promoter activity and free glucose levels for hits selected from the primary screen. *insulin* stimulators and repressors were categorized depending on whether they enhanced or reduced glucose over 20 % following treatment from 4 to 6 dpf. 84 *insulin* stimulators, which are shown in the red frame, reduced glucose, and 7 *insulin* repressors, which are shown in the blue frame, elevated glucose. (E) Results of the time course experiments. The hits were investigated over a shorter time course (12 and 24 hours) using the *Tg(ins:Luc2)* line. 32 *insulin* stimulators stimulated *insulin* promoter

activity within 12 hours. (F) Results of the secondary screening of hits for expression of *pck1*, a key regulatory gene for gluconeogenesis, with treatments from 4 to 6 dpf, using the *Tg(pck1:Luc2)* line. 13 of the 32 “12 h *insulin* stimulators” also highly stimulate *pck1* expression; they are shown as black dots in panel D. “*ins* ↑” and “*ins* ↓” indicate “*insulin* stimulators” and “*insulin* repressors”. “*pck1* ↑” and “*pck1* ↓” indicate “*pck1* stimulators” and “*pck1* repressors”. AU, arbitrary units.

Fig. 2. Functional analysis of the 5 selected *insulin* stimulators in larval zebrafish. (A) Structure of 2,4-DB, GNTI, Psora4, SR-2640 and Karanjin. (B, C and D) *Tg(ins:H2bGFP)* animals were treated with each drug starting at 4 dpf and eGFP intensity was analyzed at 6 dpf. All drugs enhanced eGFP intensity in the principal islet (mean ± STD). Scale bars, 20 μm. (E, F and G) *Tg(ins:H2bGFP)* animals were treated with each compound starting at 4 dpf and β cell numbers analyzed at 7 dpf. Psora4, SR-2640 and Karanjin increased β cell numbers in larval zebrafish. Scale bars, 20 μm. (G) Quantification of β cell numbers (mean±STD). *, P<0.05; **, P<0.01 compared to control samples by Tukey-Kramer HSD test after ANOVA.

Fig.3. Effects of the 5 *insulin* stimulators on the expression of endocrine differentiation markers. (A-F) *Tg(neurod1:eGFP)* (B and C), *Tg(pax6b:eGFP)* (D and E) and *Tg(mnx1:eGFP)* (F and G) animals were treated with each compound to investigate its effect on the expression of three genes (*neurod1*, *pax6b* and *mnx1*) involved in endocrine cell differentiation. Scale bars, 10 μm. *, P<0.05; **, P<0.01 compared to control samples by Tukey-Kramer HSD test after ANOVA.

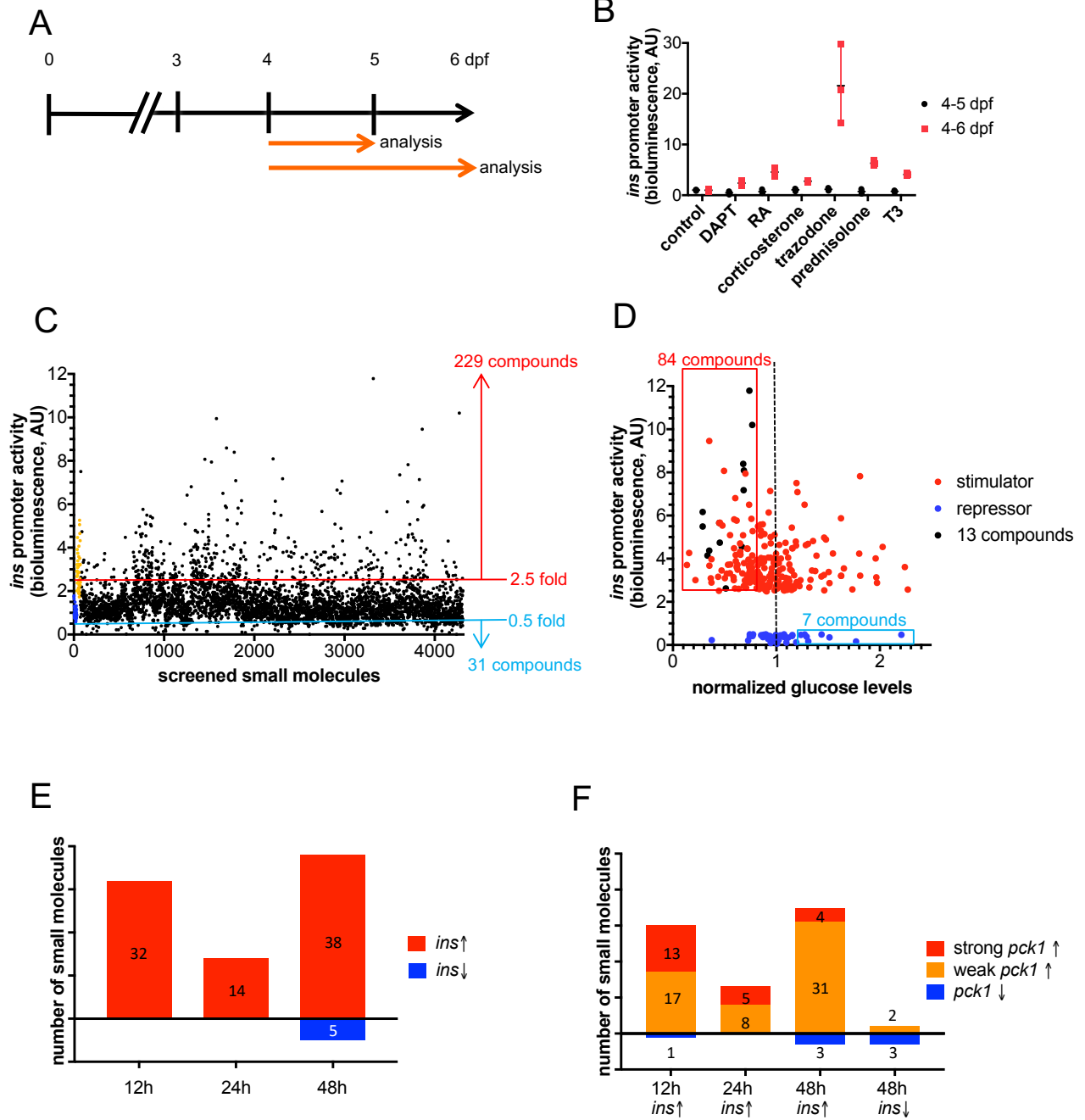
Fig. 4. Effects of the 5 *insulin* stimulators on blood glucose and blood Insulin levels in adult zebrafish. (A) Schematic time course of drug treatment. (B) Compounds were tested for their effects on blood glucose in adult zebrafish. None of the 5 compounds altered fasting blood glucose levels in adult zebrafish. However, GNTI, Psora4, SR-2640 and Karanjin, but not 2,4-DB, reduced blood glucose levels under high blood glucose condition in adults. (C and D) Effects of compounds on blood Insulin levels in adult zebrafish. All 5 compounds increased circulating Insulin levels in adult zebrafish following glucose stimulation. *, $P < 0.05$; **, $P < 0.01$ compared to control samples by Tukey-Kramer HSD test after ANOVA.

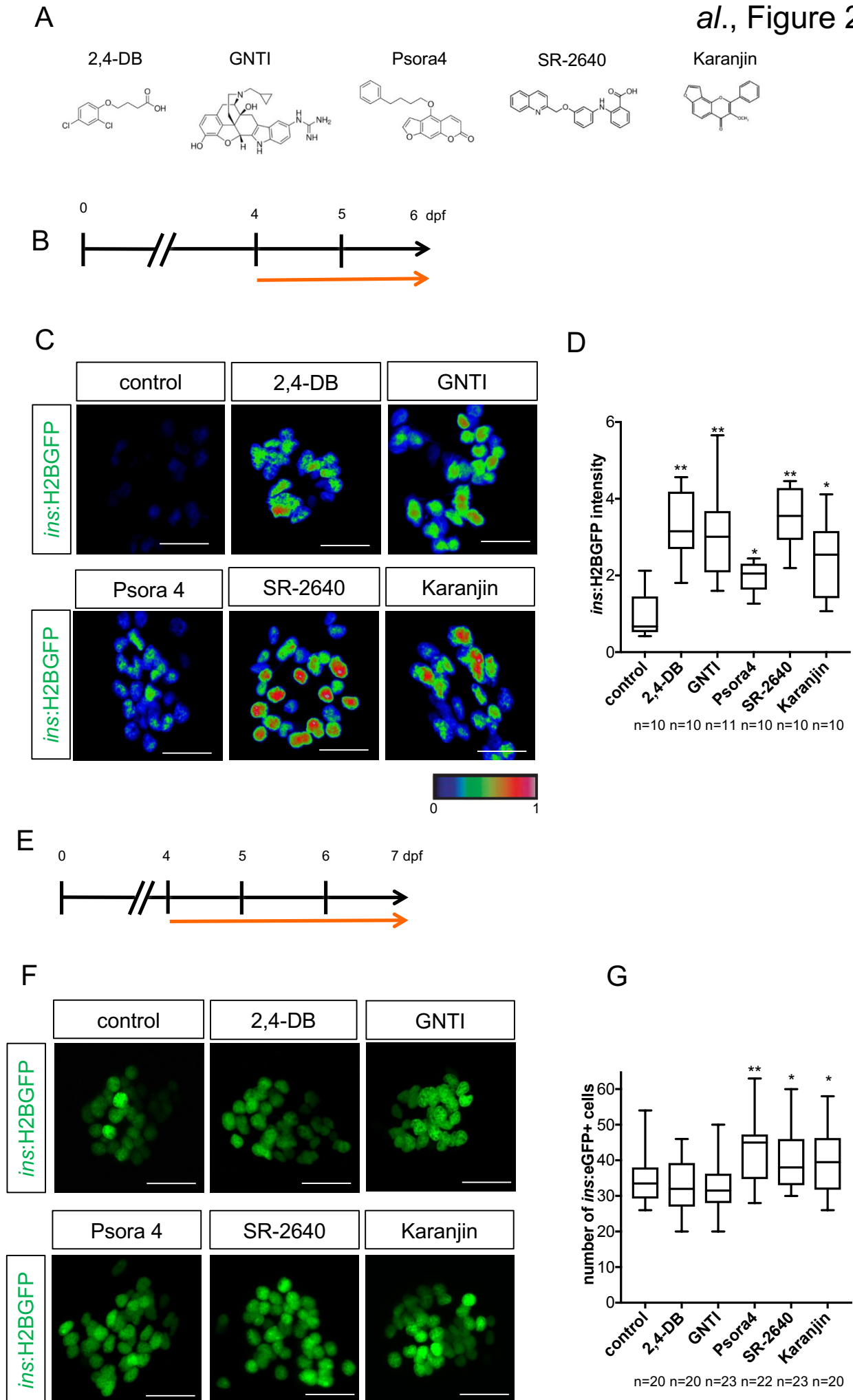
Fig. 5. Kv1.3 inhibitors stimulate Insulin secretion in mouse islets. (A) Isolated mouse islets were treated with 10 μM of the indicated compounds for 24 h and static insulin secretion assays were conducted in 3 and 15 mM glucose ($n=10$, mean \pm SEM). Potentiation of glucose stimulated insulin secretion was observed following Psora4 (Kv1.3 inhibitor) treatment. (B-C) Isolated mouse islets were treated with the 10 μM Kv1.3 inhibitors Psora4 and PAP-1 for 24 h. Static insulin secretion assays were conducted with sequential 30 min incubations in 3 mM glucose, 15 mM glucose, and 3 mM glucose ($n=8$, mean \pm SEM). Kv1.3 inhibitors consistently increased glucose stimulated insulin secretion. * $P < 0.05$; ** $P < 0.01$; *** $P < 0.001$; **** $P < 0.0001$ compared to control samples by student's t-test.

Fig. 6. Effects of Psora4 in STZ-induced hyperglycemic mice. (A) Investigation of the effects of Psora4 on blood glucose levels in STZ-induced hyperglycemic mice. IP injection of Psora4 (40 mg/kg) into mice treated with STZ (150 mg/kg) significantly reduced fasting

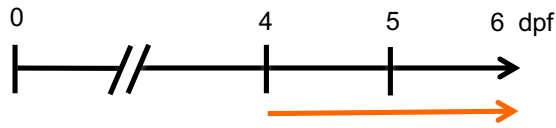
glucose levels 1 day after Psora4 injection, and Psora4-treated mice exhibited lower glucose levels than control mice (n=6, mean \pm STD). (B) AUC of each control and Psora4 sample shown in A. (C) Glucose tolerance test was performed 5 days after Psora4 injection. Blood glucose levels in mice treated with Psora4 were significantly reduced at 30 and 90 min after glucose IP injection. (D) AUC of each control and Psora4 sample shown in C. (E) Blood Insulin levels were measured after glucose injection. Blood Insulin levels increased in Psora4-treated mice 30 min after glucose IP injection. (F) Insulin tolerance test was performed at 7 days after Psora4 injection. Psora4 did not reduce blood glucose levels significantly. (G) AUC of each control and Psora4 sample shown in Fig. F. *, P<0.05; **, P<0.01 for (A), (C), (E) and (F) compared to control samples by Tukey-Kramer HSD test after ANOVA. *, P<0.05; **, P<0.01 for (B), (D), and (G) compared to control samples by student's t-test.

Fig. 7. Kv1.3 is localized mostly in the cytoplasm of pancreatic β cells in both mouse and zebrafish. Expression pattern of endogenous Kv 1.3 in adult mouse (A) and 5 dpf zebrafish (B) islets was analyzed by immunostaining. Kv1.3 is mostly localized in the cytoplasm of pancreatic β cells in both mouse and zebrafish. Notably, mouse Kv1.3 is localized in a subset of insulin granules. Scale bars, 5 μ m.

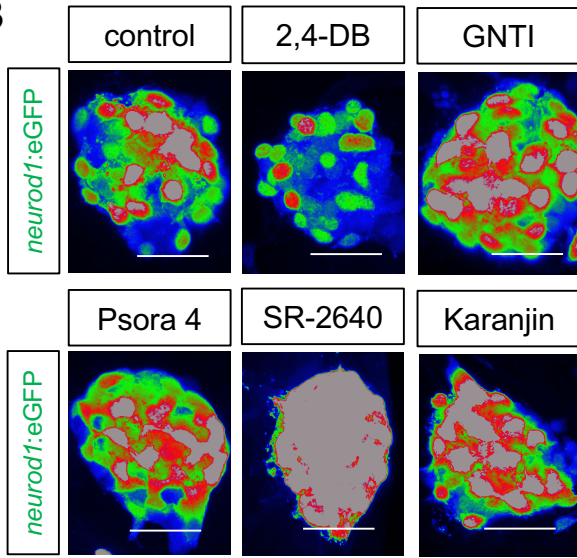


Matsuda *et al.*, Figure 2

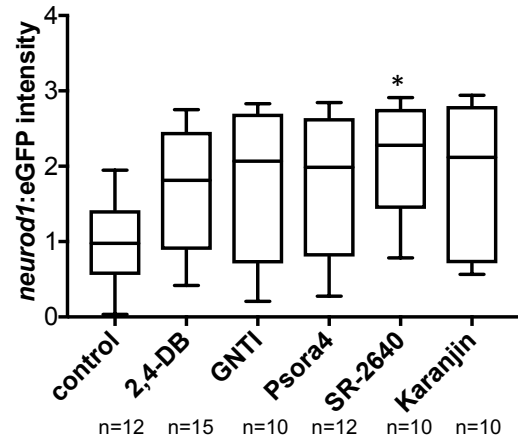
A



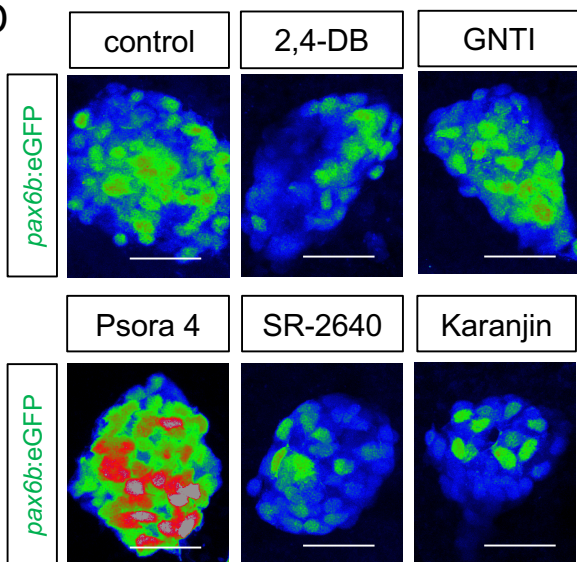
B



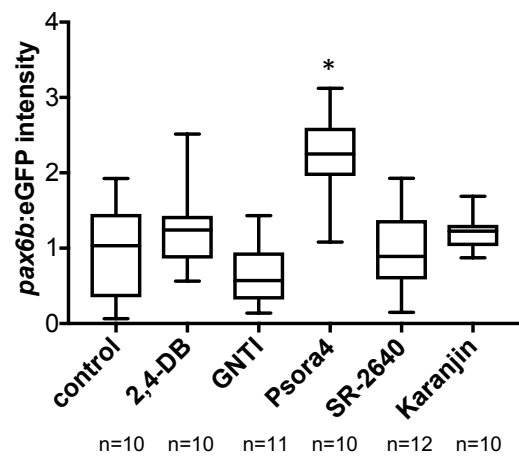
C



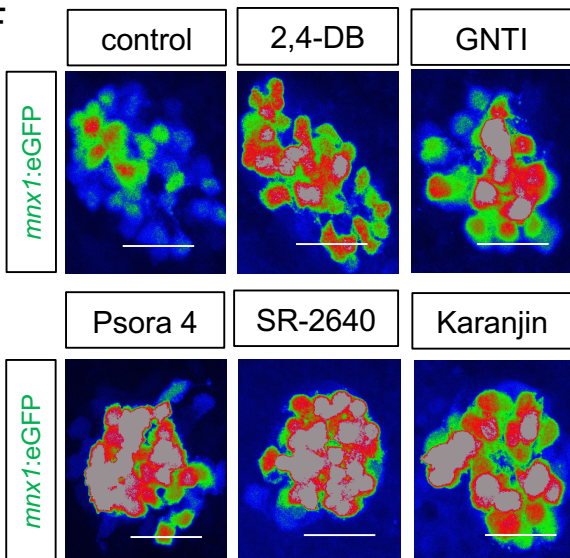
D



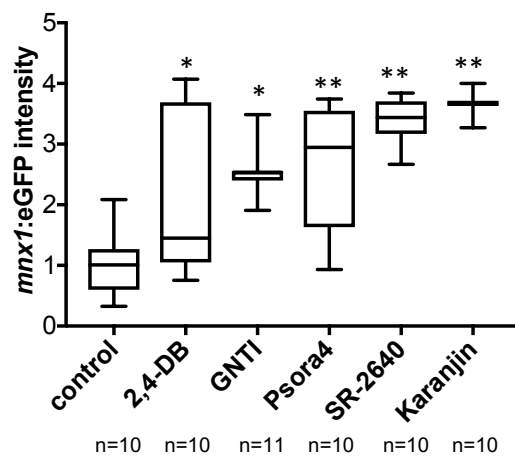
E



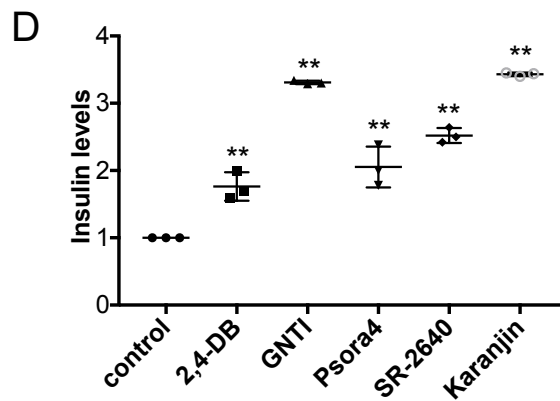
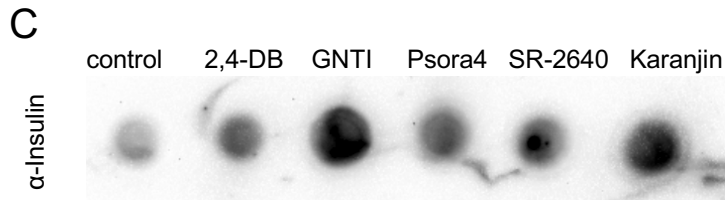
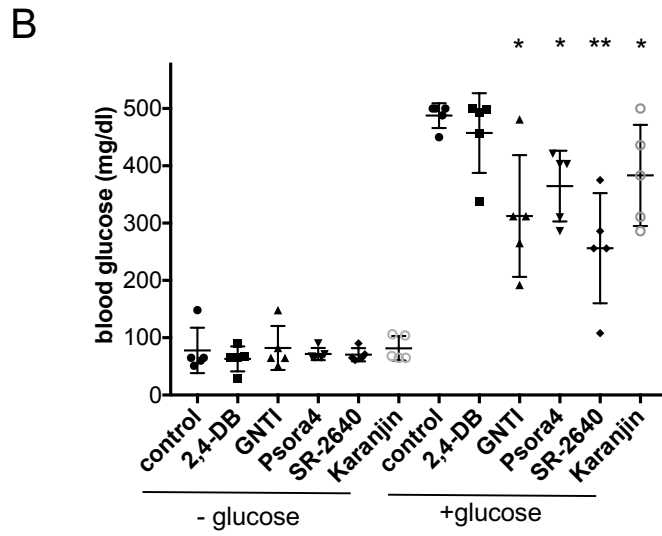
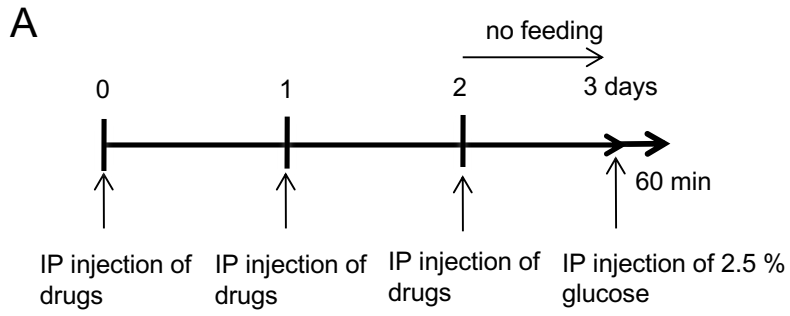
F

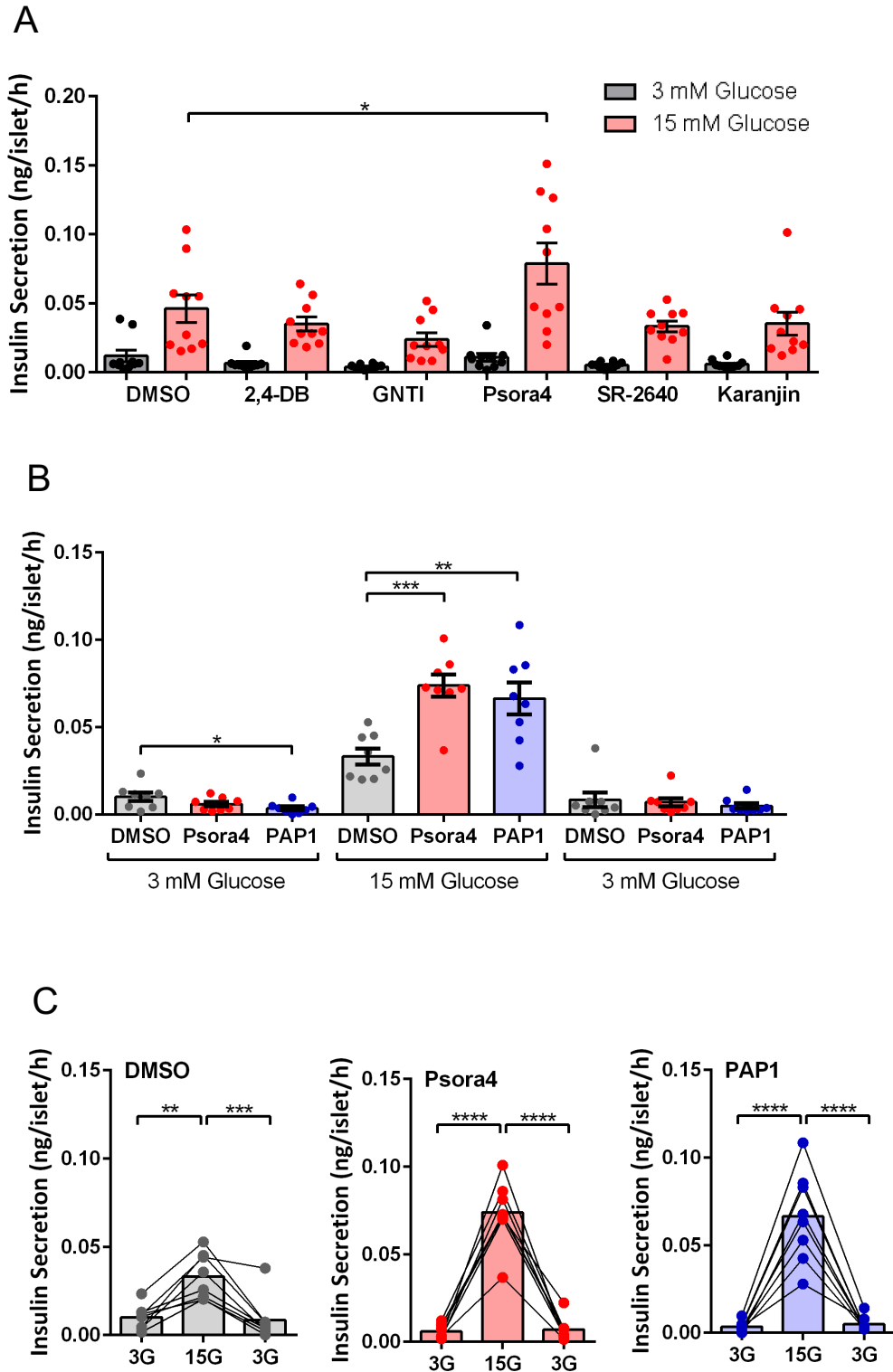


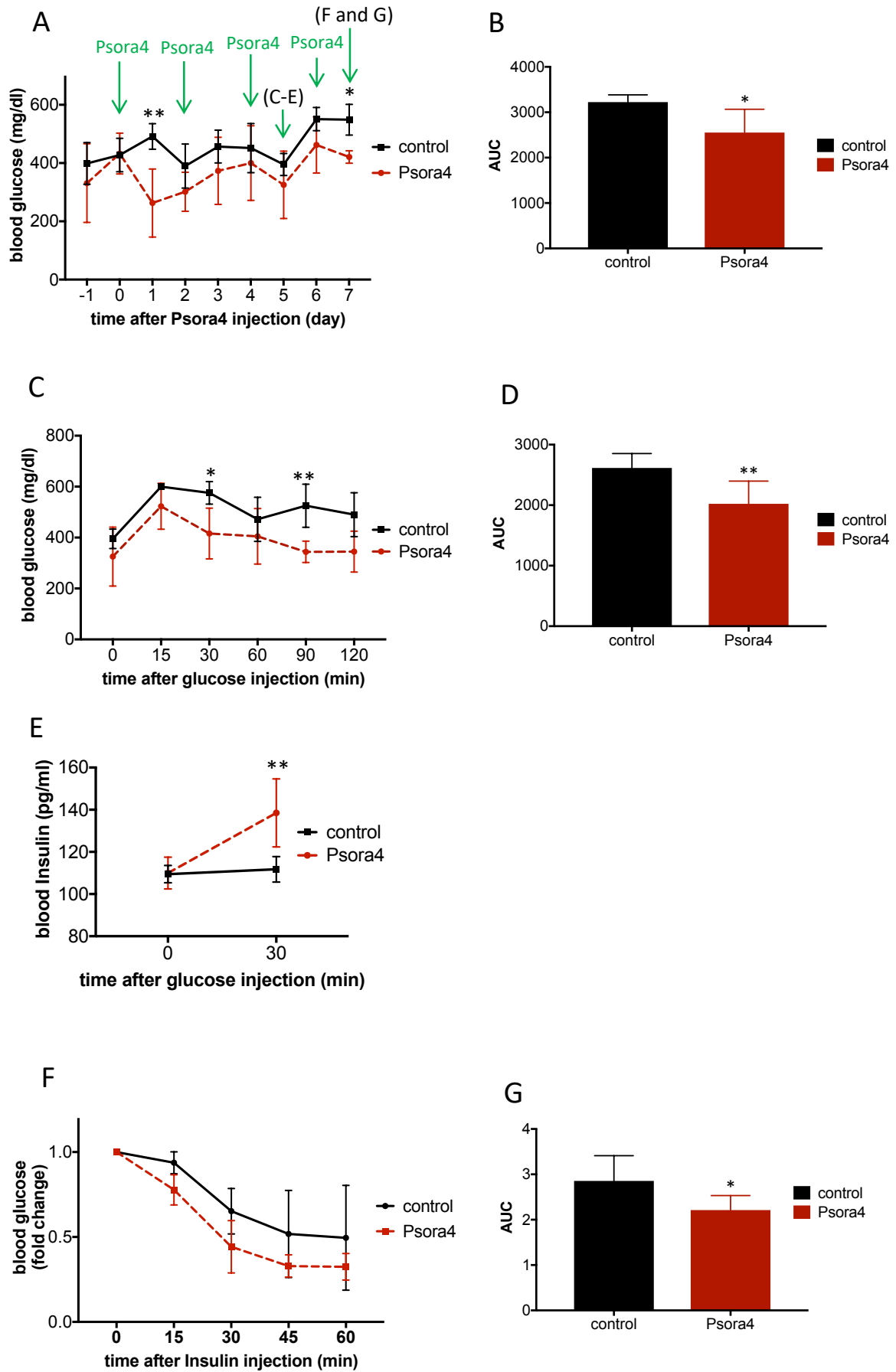
G



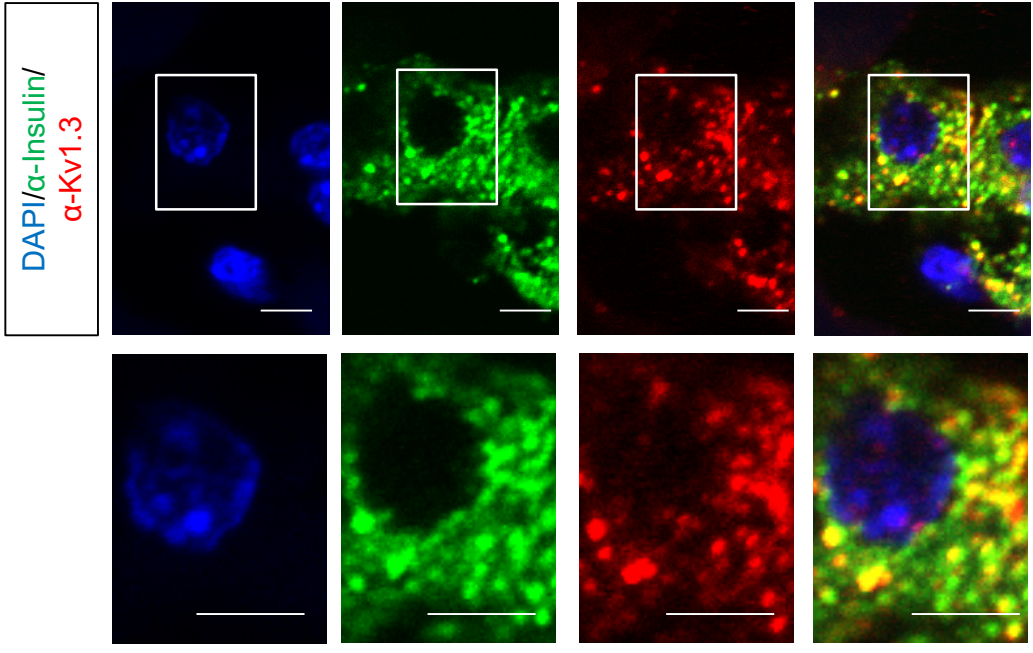
Matsuda *et al.*, Figure 4







A mouse



B zebrafish (5 dpf)

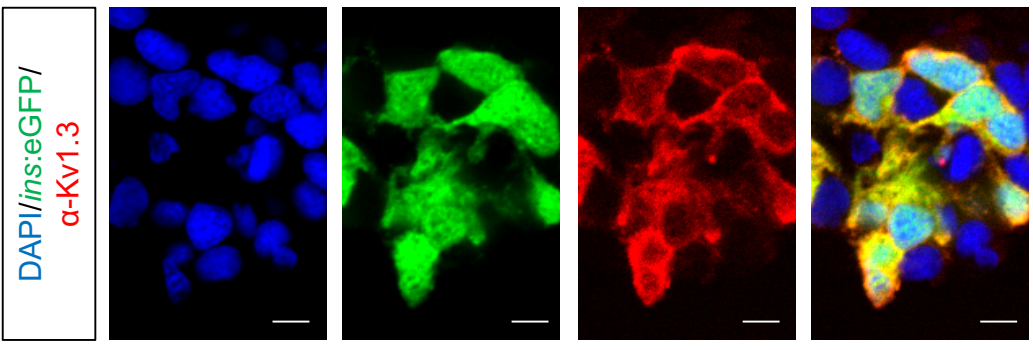


Table 1. 12 h *insulin* stimulators with high *pck1* activity (>3.5 fold)

	Name	Bioactivity	screening phenotype (fold change)		
			<i>insulin</i>	Glucose	<i>pck1</i>
1	Zardaverine	Phosphodiesterase III (PDE3) inhibitor	12.6	0.74	7.2
2	Guanidinylnaltrindole di-trifluoroacetate	κ opioid receptor antagonist	11.1	0.68	4.2
3	2,4-DICHLOROPHENOXYBUTYRIC ACID	Auxin	8.0	0.29	7.2
4	Pioglitazone	PPAR γ activator	7.6	0.73	4.0
5	Psora-4	Kv1.3 blocker	6.8	0.56	4.3
6	YM 976	Phosphodiesterase type IV (PDE4) inhibitor	5.0	0.69	4.8
7	2',4'-DIHYDROXY-4-METHOXYCHALCONE	Chalcone	5.0	0.33	4.6
8	SR-2640	LTD4/ LTE4 antagonist	3.9	0.67	3.8
9	Clorgyline hydrochloride	MAO-A inhibitor, LSD1 inhibitor	3.5	0.51	4.7
10	Octoclothepein maleate salt	Dopamine D2/serotonin 5-HT2 antagonist	3.5	0.52	7.7
11	Zotepine	Dopamine D2/serotonin 5-HT2 antagonist	2.9	0.76	6.7
12	ASARININ (-)	Lignan	2.9	0.45	3.5
13	KARANJIN	Flavonoid	2.6	0.68	5.9

Supplementary Figure 1. Assessment of *insulin* promoter activity. To determine the optimal treatment window, the effect of known stimulators of *insulin* expression was tested across various developmental windows.

Supplementary Figure 2. Dose-response curves of the effect of drugs on *insulin* promoter activity. (A) *insulin* promoter activity was enhanced by 2 or 10 μM 2,4-DB (auxin) treatment. 2,4-DB was found to be toxic at 50 μM . (B) *insulin* promoter activity was enhanced by 10 μM GNTI (KORP antagonist) treatment. GNTI was found to be toxic at 50 μM . (C) *insulin* promoter activity was enhanced by 2, 10 or 50 μM Psora-4 (Kv1.3 blocker) treatment. (D) *insulin* promoter activity was enhanced by 10 μM 2',4'-D-4-M (Chalcone) treatment. 2',4'-D-4-M was found to be toxic at 100 μM . (E) *insulin* promoter activity was enhanced by 10 or 100 μM SR-2640 (LTD4/ LTE4 antagonist) treatment. (F) *insulin* promoter activity was enhanced by 10 or 100 μM Karanjin (Flavonoid) treatment. *, $P < 0.05$; **, $P < 0.01$, ***, $P < 0.001$ compared to control samples by Tukey-Kramer HSD test after ANOVA.

Supplementary Figure 3. Dose dependent survival curves upon GNTI, 2,4-DB and 2'-4'-D-4-M treatment. Wild-type zebrafish were treated with 0, 10, 20, 40 and 50 μM 2,4-DB (A), GNTI (B) or 2'-4'-D-4-M (C) at 4 dpf and survival rate was analyzed at 4.5 dpf. We removed 2'-4'-D-4-M from the drugs which we characterized further due to its high toxicity.

Supplementary Figure 4. Effects of the 5 *insulin* stimulators on the expression of pancreatic endocrine markers in zebrafish larvae. Wild-type fish were treated with each compound at 4 dpf and the expression of *insulin* and indicated endocrine genes was analyzed at 4.5 (A) and 6 (B) dpf by qPCR (mean±STD). All compounds stimulated endogenous *insulin* expression at 4.5 and 6 dpf. *, P<0.05; **, P<0.01 compared to control samples by Tukey-Kramer HSD test after ANOVA.

Supplementary Figure 5. Effects of the 5 *insulin* stimulators on the expression of pancreatic endocrine markers in adult. Adult wild-type fish were IP injected with each drug once a day for three consecutive days, and the expression of *insulin* and indicated endocrine genes was analyzed by qPCR at 24 hours after the last injection (mean±STD). *, P<0.05; **, P<0.01 compared to control samples by Tukey-Kramer HSD test after ANOVA.

Supplementary Figure 6. Effects of the 5 selected *insulin* stimulators on the expression of endocrine differentiation markers in the principal islet at 4.5 dpf. (A-C)

Tg(neurod1:eGFP) (A), *Tg(pax6b:eGFP)* (B) and *Tg(mnx1:eGFP)* (C) animals were treated with each compound at 4 dpf and analyzed for eGFP intensity in the principal islet at 4.5 dpf. Scale bars, 10 µm. *, P<0.05; **, P<0.01 compared to control samples by Tukey-Kramer HSD test after ANOVA.

Supplementary Figure 7. Kv1.3 inhibitors stimulate *insulin* expression and β cell

numbers in larval zebrafish as well as Insulin secretion in adult zebrafish. (A) Zebrafish were treated with 1 μ M Psora4 or indicated concentration of PAP-1 or clafozamine at 4 dpf and analyzed at 4.5 dpf for *insulin* promoter activity. *insulin* promoter activity was enhanced by 10 μ M PAP-1 as well as 10 μ M clafozamine. Both PAP-1 and clafozamine were found to be toxic at 100 μ M. (B) Wild-type fish were treated with 10 μ M PAP-1 or 10 μ M clafozamine at 4 dpf and *insulin* expression was analyzed at 4.5 dpf by qPCR. (C-E) *Tg(ins:eGFP)* animals were treated with 10 μ M PAP-1 starting at 4 dpf and analyzed at 7 dpf. Note that β cell numbers increased with PAP-1 treatment (C and D) and that eGFP intensity was enhanced after PAP-1 treatment (C and E). (F) PAP-1 and clafozamine were tested for their effect on blood glucose levels in adult zebrafish. PAP-1 and clafozamine did not alter fasting blood glucose levels in adult zebrafish. However, both compounds reduced blood glucose levels under high blood glucose condition in adults. (G and H) Effects of PAP-1 and clafozamine on blood Insulin levels in adult zebrafish. PAP-1 and clafozamine increased circulating Insulin levels in adult zebrafish following glucose stimulation. *, $P < 0.05$; **, $P < 0.01$ compared to control samples in (A), (B), (F) and (H) by Tukey-Kramer HSD test after ANOVA and in (D) and (E) by Student t-test.

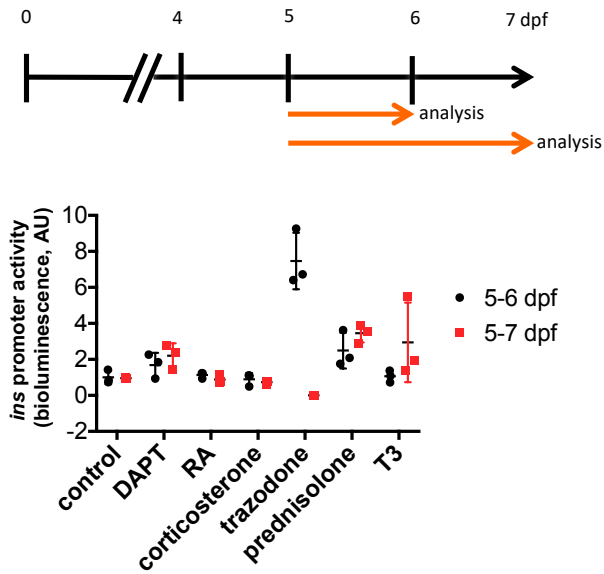
Supplementary Figure 8. Dose dependent survival curves upon treatment with Kv 1.3

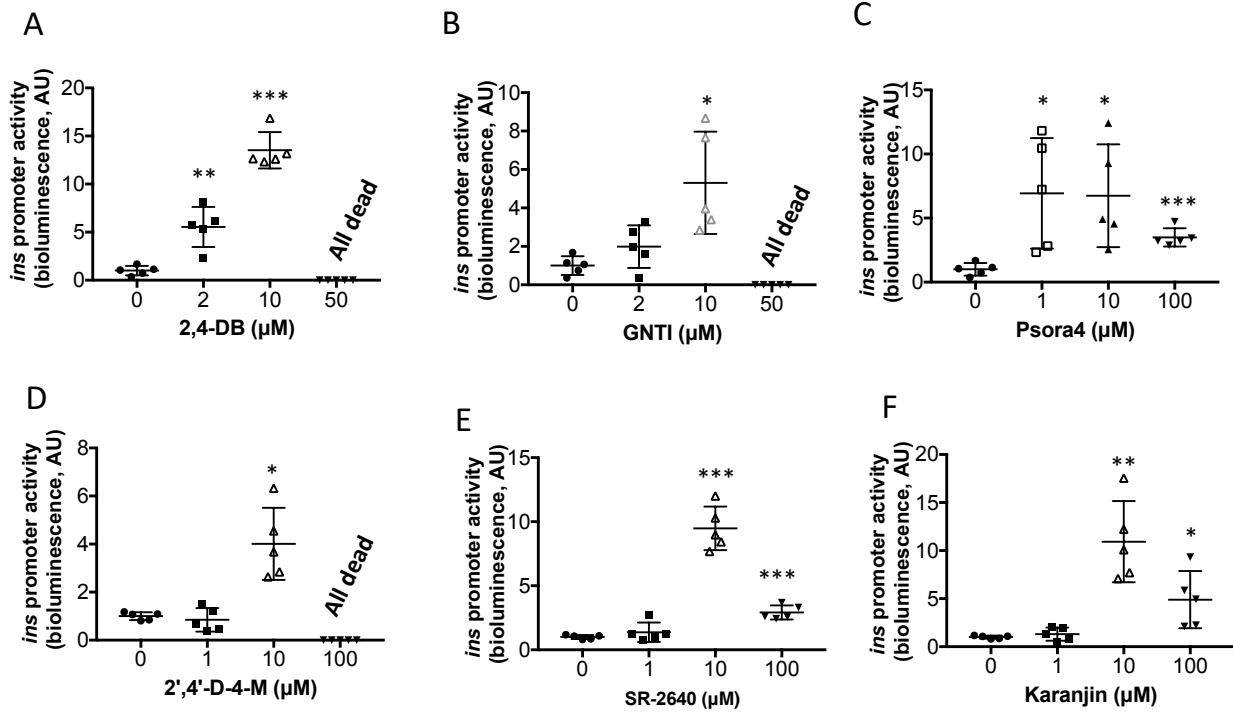
inhibitors. Wild-type zebrafish were treated with 0, 10, 20, 40 and 50 μ M Psora4 (A), PAP-1 (B) or clafozamine (C) at 4 dpf and survival rate was analyzed at 4.5 dpf. PAP-1 and clafozamine showed higher toxicity than Psora-4.

Supplementary Figure 9. Effect of Kv 1.3 inhibitors on the expression of pancreatic endocrine markers in isolated mouse islets. (A-B) Isolated mouse islets were treated with 10 μ M Kv1.3 inhibitors, Psora4 and PAP-1, for 24 h. qRT-PCR revealed down-regulation of *Ins1* expression and up-regulation of *Ins2* expression following PAP-1 treatment (B). (n=11, mean \pm SEM). *, P<0.05 compared to DMSO treatment by student's t-test.

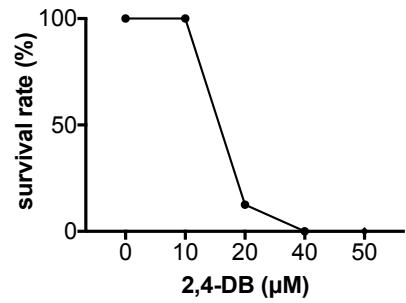
Supplementary Figure 10. Amino acid sequence comparison of the Kv1.3 antibody target region between mouse and zebrafish. C-terminal region of Kv1.3, which is the target of the antibody, was compared between mouse (amino acid residues 478-530) and zebrafish (amino acid residues 475-515). 31 amino acids are conserved between mouse and zebrafish.

Matsuda *et al.*,
Supplement
Figure 1

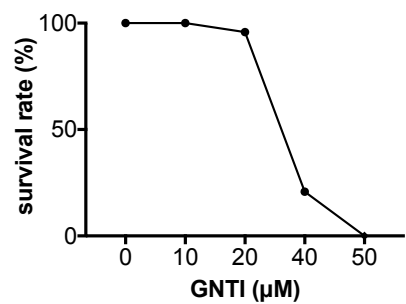


Matsuda *et al.*,
Supplement
Figure 2

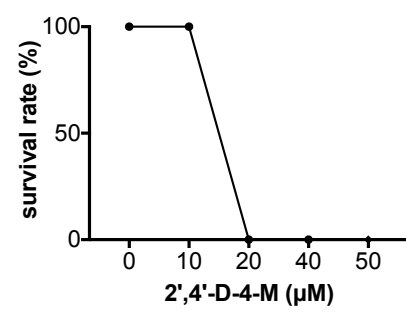
A



B



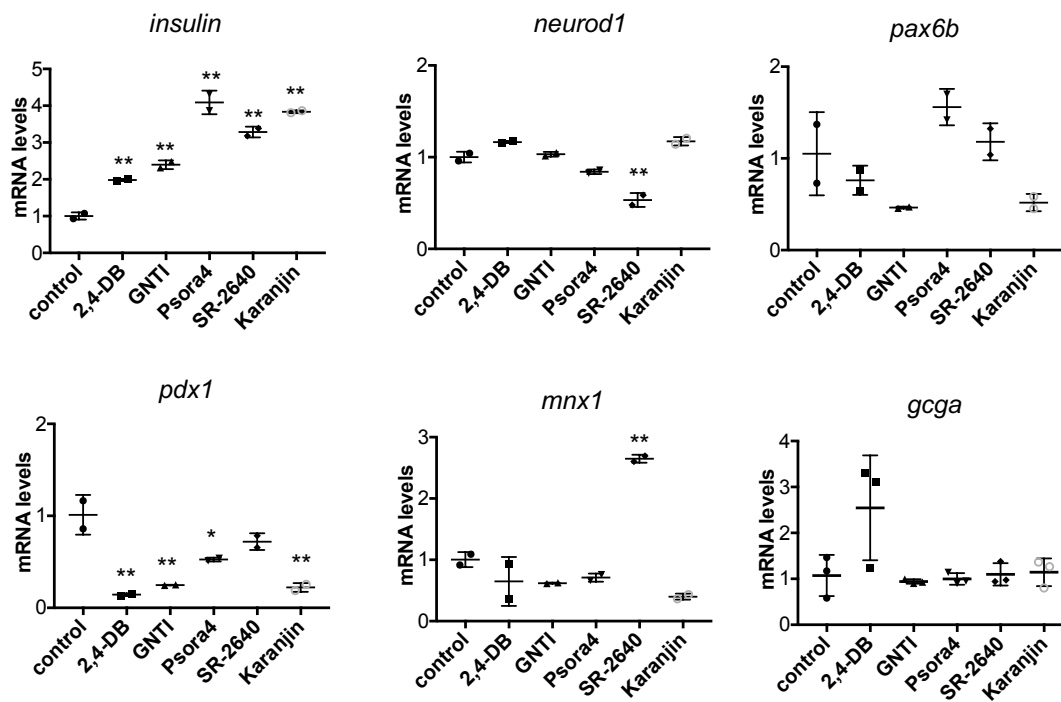
C



Matsuda *et al.*,
Supplement
Figure 4

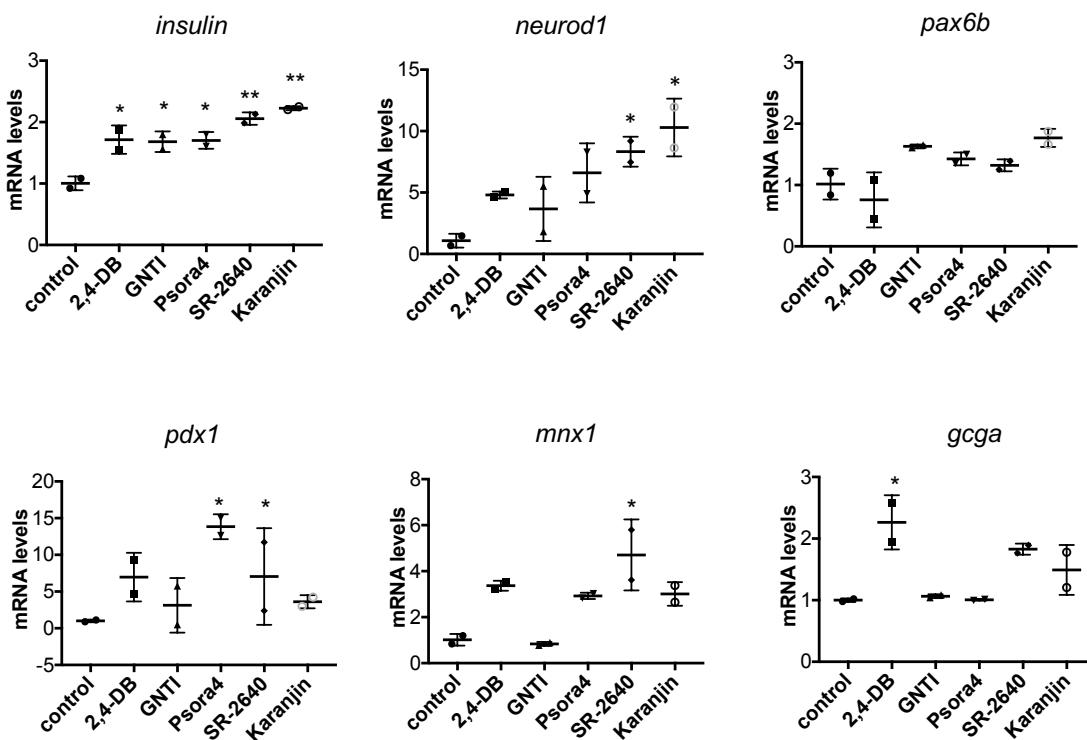
A

4.5 dpf

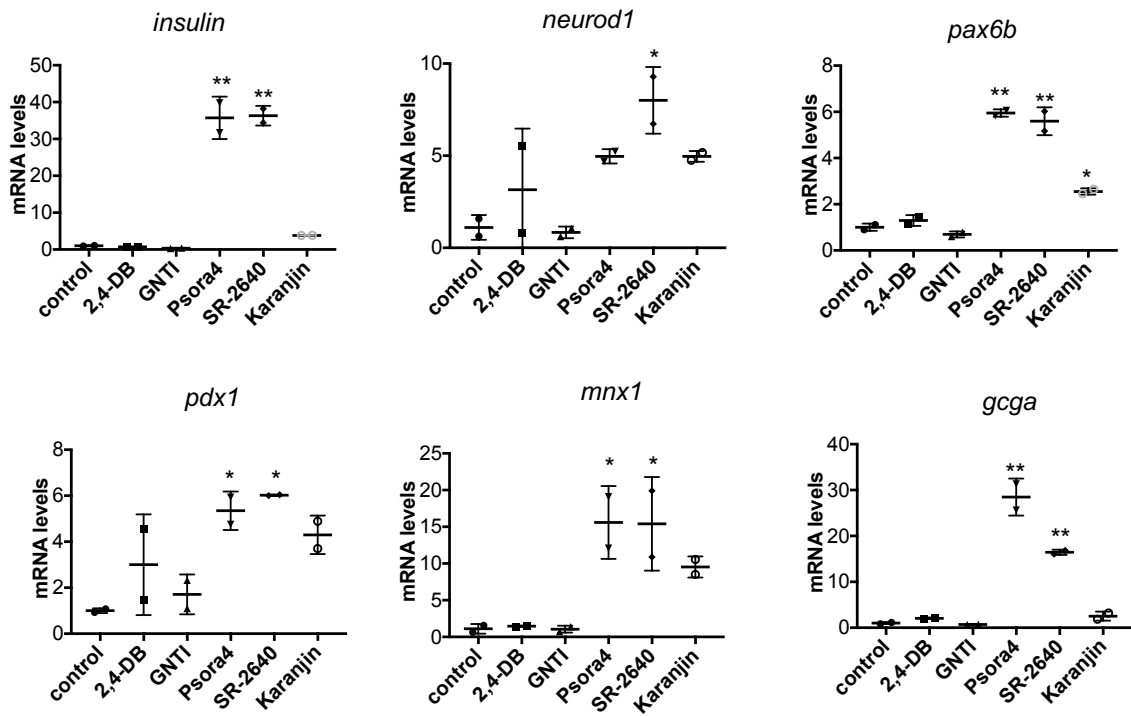


B

6 dpf

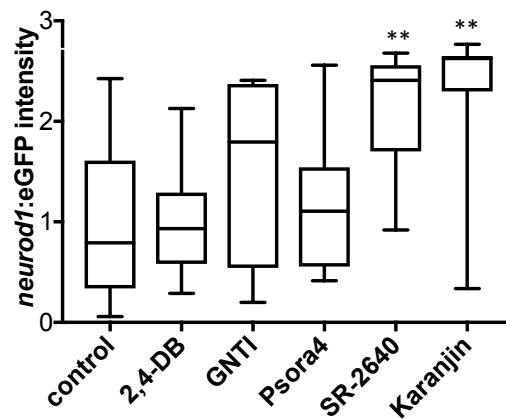
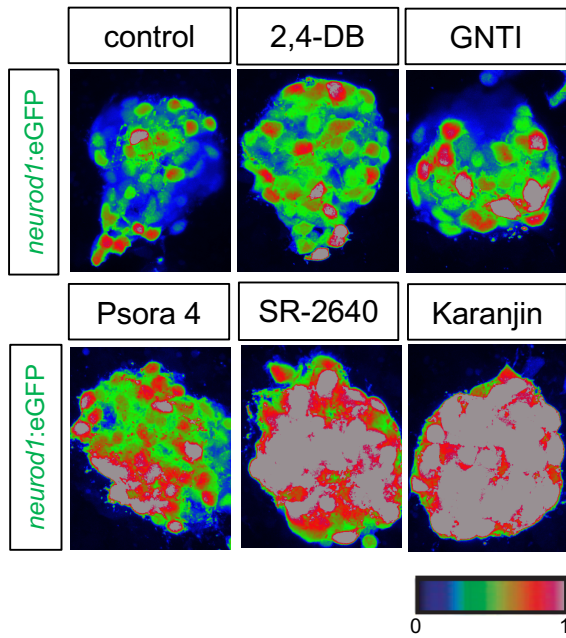


adult

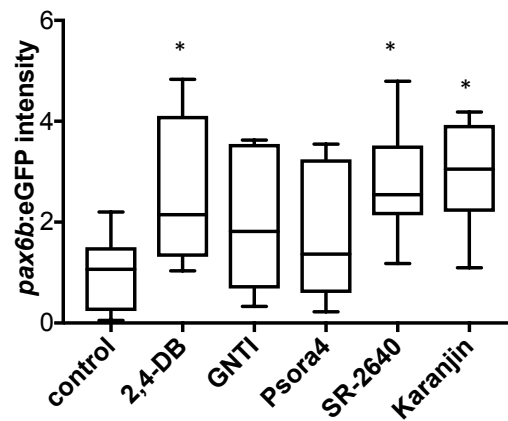
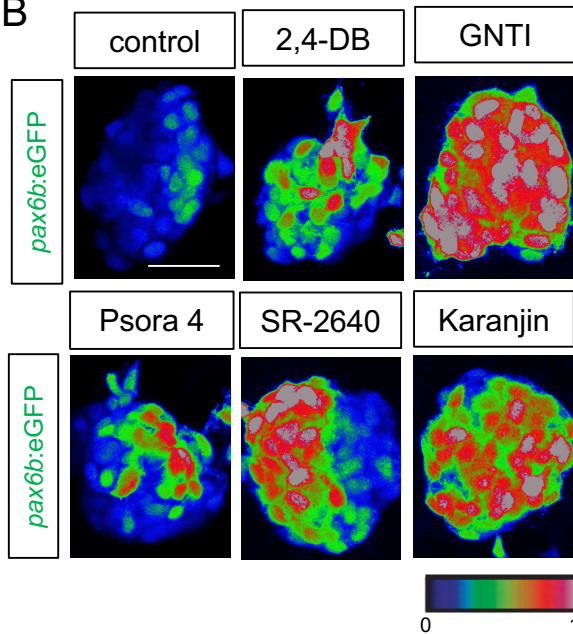


Matsuda *et al.*,
supplement
Figure 6

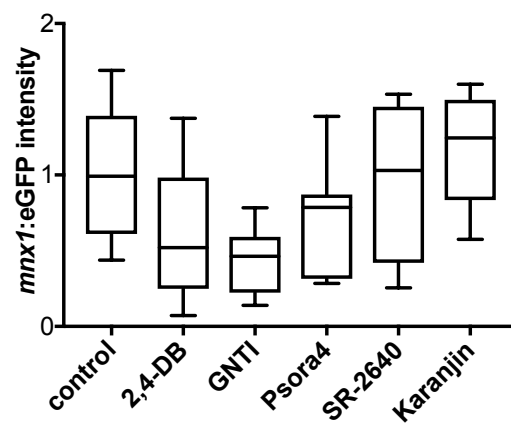
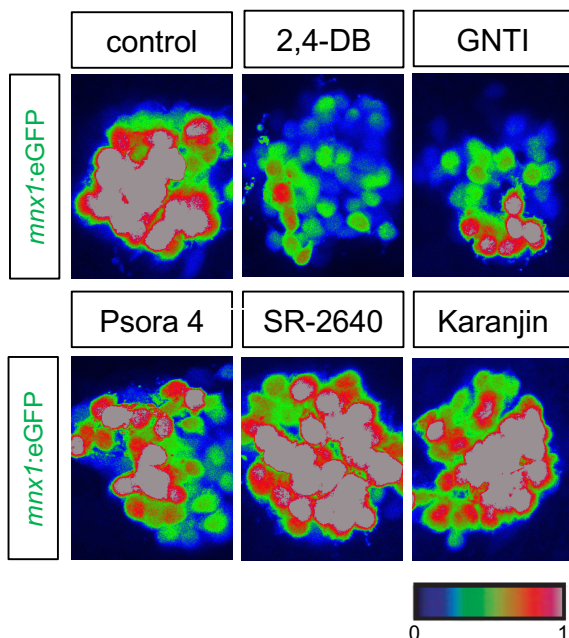
A

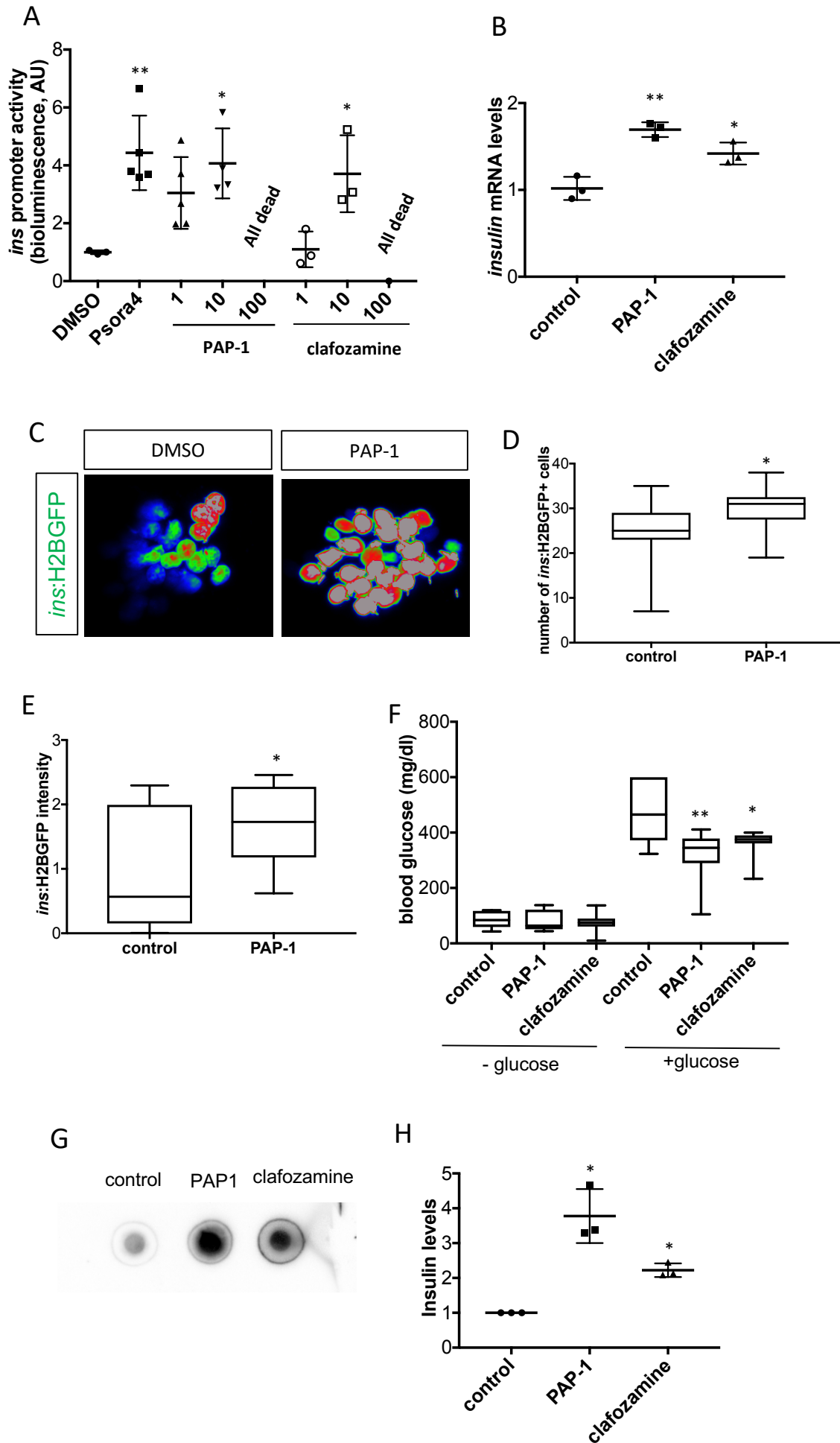


B



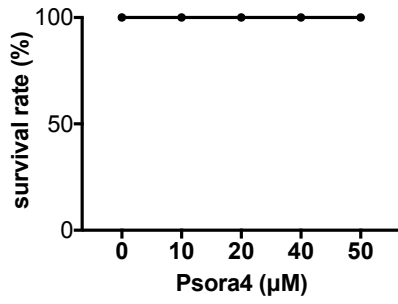
C



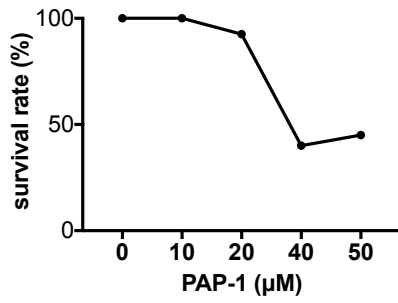


Matsuda *et al.*,
Supplement
Figure 8

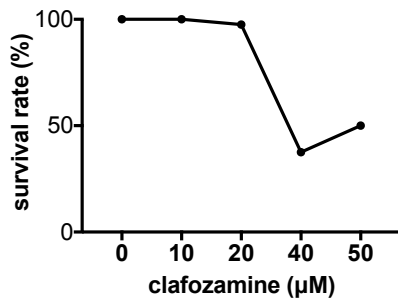
A

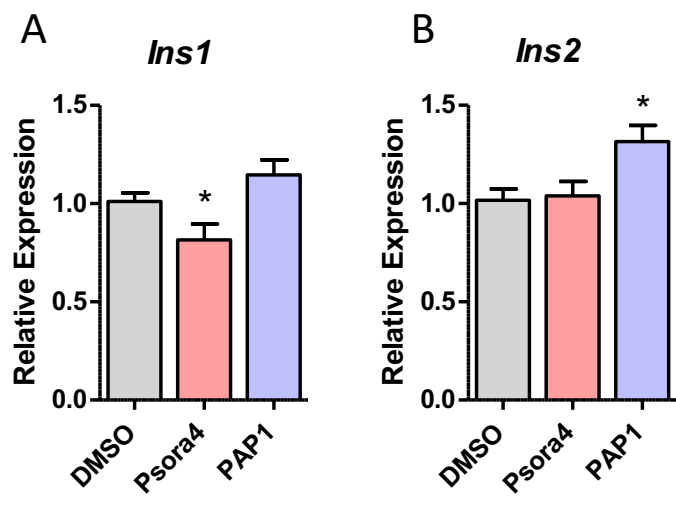


B



C





Matsuda *et al.*,
Supplement
Figure 10

```
mouse      T L S K S E Y M V I E E G G M N H S A F P Q T P F K T G N S T A T C T T N N N P N S C V N I K K I F T D V
zebrafish  S L S K S E Y M V I E E G -- I N S A F K Q - P ----- N Y S N Q N N Q N C V N I K K I F T D V
          *****          * * * * *          * *          *****
```

Supplementary table 1. List of 12 h *insulin* stimulators

12 h <i>insulin</i> stimulators with moderate <i>pck1</i> activity (1<3.5 fold)			screening phenotype (fold change)		
	Name	Bioactivity	<i>insulin</i>	Glucose	<i>pck1</i>
1	POLYMYXIN B SULFATE	antibacterial	2.5	0.35	2.3
2	BICUCULLINE(-) METHIODIDE	GABAa antagonist	2.7	0.77	2.6
3	PANCURONIUM BROMIDE	Aminosteroidal neuromuscular blocking agent	2.8	0.63	2.5
4	YC-1	NO (nitric oxide)-independent activator of soluble guanylyl	2.8	0.81	2.2
5	HARMINE	MAO inhibitor	3.0	0.68	3.5
6	2',5'-DIHYDROXY-4-METHOXYCHALCONE	Flavonoid	3.0	0.49	2.9
7	SINENSETIN	Flavonoid, iNOS inhibitor and Cox2 inhibitor, TNF-alpha inh	3.2	0.48	2.3
8	Quazinone	Phosphodiesterase III (PDE3) inhibitor	3.2	0.76	3.2
9	FLUTAMIDE	antiandrogen	3.3	0.47	2.0
10	DEMETHYLNOBILETIN	citrus flavonoid	3.4	0.37	3.1
11	K 185	Melatonin receptor antagonist	3.6	0.73	2.4
12	SP600125	inhibitor of c-Jun N-terminal kinase (JNK)	4.7	0.63	3.2
13	HEXAMETHYLQUERCETAGETIN	PIM1 kinase antagonist	5.0	0.65	2.1
14	TICLOPIDINE HYDROCHLORIDE	ADP receptor blocker	5.0	0.79	3.0
15	DILOXANIDE FUROATE	amoebicide	5.2	0.69	2.6
16	Kenpauillone	potent inhibitor of CDK1/cyclin B	7.9	0.68	2.5
17	Liranaftate	antifungal	11.7	0.80	2.9

12 h <i>insulin</i> stimulators with low <i>pck1</i> activity (<1 fold)			screening phenotype (fold change)		
	Name	Bioactivity	<i>insulin</i>	Glucose	<i>pck1</i>
1	IC 261	Casein kinase 1 δ (CK1 δ) and CK1 ϵ inhibitor	4.5	0.71	0.9

12 h <i>insulin</i> stimulators (no <i>pck1</i> results)			screening phenotype (fold change)		
	Name	Bioactivity	<i>insulin</i>	Glucose	<i>pck1</i>
1	(\pm)-Bay K8644	calcium channel agonist	5.1	0.71	-

Supplementary table 2. List of 24 h *insulin* stimulators

24 h <i>insulin</i> stimulators with moderate <i>pck1</i> activity (>3.5 fold)			screening phenotype (fold change)		
	Name	Bioactivity	<i>insulin</i>	Glucose	<i>pck1</i>
1	LARIXOL ACETATE		3.8	0.14	4.7
2	ANAGRELIDE HYDROCHLORIDE	Phosphodiesterase 3 (PDE3) inhibitor	3.0	0.71	5.9
3	3,7-DIMETHOXYFLAVONE	Flavonoid	2.8	0.60	5.7
4	4-METHYLESCULETIN	antioxidant	2.6	0.52	4.2
5	BERGAPTEN	antipsoriatic, antiinflammatory	2.5	0.52	7.4

24 h <i>insulin</i> stimulators with moderate <i>pck1</i> activity (1<3.5 fold)			screening phenotype (fold change)		
	Name	Bioactivity	<i>insulin</i>	Glucose	<i>pck1</i>
1	CARNOSIC ACID	antioxidant lipid peroxidation inhibitor, PPAR gamma activator	6.6	0.74	2.5
2	3-METHOXYCATECHOL	converted 3-methylcatechol into acetaldehyde and pyruvate	4.8	0.70	1.9
3	TRIPTOPHENOLIDE	diterpenoid	4.1	0.59	3.2
4	XANTHONE	Aromatic Ketone	4.0	0.72	2.9
5	DICHLORODIPHENYLDICHLOROETHYLENE	insecticide	3.8	0.75	1.5
6	MANGOSTIN TRIMETHYL ETHER		2.9	0.73	2.1
7	TERBINAFINE HYDROCHLORIDE	Inhibits squalene epoxidase, preventing biosynthesis of ergosterol	2.9	0.67	2.4
8	PTERYXIN	muscle relaxant	2.7	0.71	2.2

24 h <i>insulin</i> stimulators (no <i>pck1</i> results)			screening phenotype (fold change)		
	Name	Bioactivity	<i>insulin</i>	Glucose	<i>pck1</i>
1	ENTANDROPHRAGMIN		3.2	0.65	-

Supplementary table 3. List of 48 h *insulin* stimulators

48 h <i>insulin</i> stimulators with modetate <i>pck1</i> activity (>3.5 fold)			screening phenotype (fold change)		
Name	Bioactivity	<i>insulin</i>	Glucose	<i>pck1</i>	
1 Mitotane	anti-adrenocorticoid	9.5	0.35	4.3	
2 REBAMIPIDE	antiulcer, antioxidant	5.8	0.76	5.0	
3 1-Phenyl-3-(2-thiazolyl)-2-thiourea	Dopamine β -hydroxylase inhibitor	4.5	0.72	8.1	
4 SPHONDIN	NF-kappaB inhibitor , Cox inhibitor	3.2	0.44	3.7	

48 h <i>insulin</i> stimulators with modetate <i>pck1</i> activity (1<3.5 fold)			screening phenotype (fold change)		
Name	Bioactivity	<i>insulin</i>	Glucose	<i>pck1</i>	
1 FARNESOL	anti-bacterial	5.8	0.77	2.7	
2 SECURININE	GABAA receptor blocker, CNS stimulant	4.5	0.76	1.4	
3 ISOXICAM	Cyclooxygen inhibitor	4.5	0.72	2.1	
4 Norgestimate	progestogen	4.3	0.65	3.5	
5 Mephetyl tetrazole	Kv1.5 potassium channel blocker	4.3	0.16	2.1	
6 CURCUMIN	PAIN 'antiedemic, antiinflammatory, bile stimulant;	4.2	0.61	1.6	
7 PRIMULETIN	Flavonoid	4.2	0.77	1.2	
8 PERILLYL ALCOHOL	antineoplastic, apoptosis inducer	3.9	0.69	1.6	
9 COUMOPHOS	insecticide, cholinesterase inhibitor	3.9	0.61	1.6	
10 DCEBIO	activating K+ and Cl- currents	3.7	0.56	2.1	
11 DICHLORVOS	insecticide, cholinesterase inhibitor	3.7	0.62	3.1	
12 5-HYDROXY-2',4',7,8-TETRAMETHOXYFLAVONE	flavonoid	3.7	0.53	1.2	
13 PIZOTYLINE MALATE	Serotonin receptor antagonist	3.6	0.77	2.9	
14 PHENYLBUTAZONE	Cyclooxygen inhibitor	3.4	0.76	1.3	
15 ARTEMISININ	antimalarial	3.4	0.74	2.8	
16 L-745,870 hydrochloride	Selective D4 dopamine receptor antagonist	3.3	0.73	2.5	
17 NEROL	monoterpene	3.3	0.74	1.4	
18 HUMULENE (alpha)	TNF- α ,IL-1 β inhibitor	3.2	0.71	1.2	
19 Piroxicam	Cyclooxygen inhibitor	3.2	0.79	2.9	
20 ATRAZINE	herbicide	3.1	0.74	1.6	
21 CRYPTOTANSHINONE	Stat3 inhibitor	3.1	0.65	1.6	
22 Benperidol	Dopamine antagonist	3.1	0.74	1.7	
23 CRESOL	antiinfectant	3.1	0.72	1.4	
24 CHLOROTRIANISENE	estrogen	3.0	0.59	2.9	
25 DIFLUNISAL	Cyclooxygenase inhibitor	3.0	0.79	1.4	
26 LEVOTHYROXINE	Thyroid hormone	3.0	0.32	2.3	
27 TRIADIMEFON	P450 inhibitor	3.0	0.70	1.8	
28 CORYNANTHINE	alkaloid	2.9	0.80	1.3	
29 CHLORTHALIDONE	Sodium-chloride symporter inhibitor	2.8	0.69	1.8	
30 Imperatorin	a modulator of p38, ERK pathway	2.6	0.60	1.3	
31 GUAIAZULENE	antioxidant, inhibits lipid peroxidation inhibitor,	2.6	0.76	1.3	

48 h <i>insulin</i> stimulators with low <i>pck1</i> activity (<1 fold)			screening phenotype (fold change)		
---	--	--	-----------------------------------	--	--

	Name	Bioactivity	<i>insulin</i>	Glucose	<i>pck1</i>
1	Picrotoxin	GABA _A receptor antagonist; binds to the GABA receptor-link	4.0	0.75	1.0
2	PD 169316	p38 MAP kinase inhibitor	3.8	0.69	0.6
3	TRICHLORFON	Acetylcholinesterase inhibitor	2.7	0.68	0.9

Supplementary table 4. List of *insulin* repressors

48 h <i>insulin</i> repressors with moderate <i>pck1</i> activity (1<3.5 fold)			screening phenotype (fold change)		
	Name	Bioactivity	<i>insulin</i>	Glucose	<i>pck1</i>
1	Levallorphan tartrate salt	Partial agonist (antagonist) at μ and δ opioid receptors	0.49	1.33	1.89
2	A-68930 hydrochloride	Selective D ₁ dopamine receptor agonist	0.47	1.24	1.28

48 h <i>insulin</i> repressors with low <i>pck1</i> activity (<1 fold)			screening phenotype (fold change)		
	Name	Bioactivity	<i>insulin</i>	Glucose	<i>pck1</i>
1	N-(3,3-Diphenylpropyl)glycinamide	NMDA glutamate receptor open channel blocker	0.49	1.25	0.96
2	TPCA-1	I κ B kinase-2 inhibitor	0.35	1.51	0.77
3	5-Fluoro-5'-deoxyuridine	thymidylate synthase inhibitor	0.38	1.27	0.72

. . .

. . .

Supplementary Table 5. primers sequence for qPCR

primer name	sequence (5'-->3')	reference
<i>insulin</i> -f	TTTAAATGCAAAGTCAGCCACCTCAG	44
<i>insulin</i> -r	GGCTTCTTCTACAACCCCAAGAGAGA	44
<i>neurod1</i> -f	CTTTC AACACACCCTAGAGTTCCG	13
<i>neurod1</i> -r	GCATCATGCTTTCCTCGCTGTATG	13
<i>pax6b</i> -f	GCCAGGACAACCAAATCAAGACG	13
<i>pax6b</i> -r	GTGAAGGACGTTCTGTTTCTCTGC	13
<i>pdx1</i> -f	CACAGGACCAGCCAAATCTT	
<i>pdx1</i> -r	GTGAAGTTTGGGGAAGGTGA	
<i>isl1</i> -f	CAACACGCCATGATAACGAC	45
<i>isl1</i> -r	AGCAGCAGCAACCCAACGACA	45
<i>pax4</i> -f	GAGAGAGCCTGCAGAGGAGA	13
<i>pax4</i> -r	TGTTGCTGAAAATGGCTCTG	13
<i>mnx1</i> -f	GAAGAGGAGCGGTGACACTC	13
<i>mnx1</i> -r	GGTCTGCACTTTTGGTGGAT	13
<i>ucn3l</i> -f	ACGCAGCCAGGTC ACTCTAT	
<i>ucn3l</i> -r	GTTCTTGGCTTTGGCAATGT	
<i>actb</i> -f	GTGGTCTCGTGGATACCGCAA	44
<i>actb</i> -r	CTATGAGCTGCCTGACGGTCA	44

Supplementary Table 6. Cq value of qPCR**4.5 dpf**

<i>actb</i>	Cq
control	24.77
	24.97
24DB	24.87
	24.9
GNTI	24.92
	24.86
Psora4	24.94
	24.79
SR2640	24.68
	24.92
Karanjin	24.94
	24.76
<i>ins</i>	
control	32
	32.2
24DB	31.13
	31.1
GNTI	30.89
	30.79
Psora4	30.15
	29.99
SR2640	30.43
	30.34
Karanjin	30.15
	30.17
<i>neurod1</i>	
control	28.12
	28.24
24DB	27.97
	27.95
GNTI	28.11
	28.16
Psora4	28.4
	28.46
SR2640	28.95
	29.24
Karanjin	27.99
	27.91
<i>pax6b</i>	
control	30.95
	30.04
24DB	30.69

	31.12
GNTI	31.58
	31.63
Psora4	29.99
	29.73
SR2640	30.44
	30.09
Karanjin	31.27
	31.64
<i>pdx1</i>	
control	27.63
	27.19
24DB	30.11
	30.31
GNTI	29.44
	29.41
Psora4	28.3
	28.38
SR2640	27.76
	28.02
Karanjin	29.38
	29.82
<i>mnx1</i>	
control	28.92
	28.67
GNTI	29.44
	29.41
24DB	30.57
	30.76
Psora4	29.33
	29.14
SR2640	27.34
	27.39
Karanjin	30.26
	30.01
<i>acta</i>	
control	24.15
	23.49
	23.77
24DB	24.06
	23.78
	23.76
GNTI	24.05
	23.77
	23.77
Psora4	24.1

	23.72
	23.77
SR2640	24.23
	23.8
	23.55
Karanjin	24.38
	23.62
	23.6
<i>gcga</i>	
control	35.6
	34.27
	34.59
24DB	35.39
	33.97
	34.06
GNTI	39.06
	38.96
	39.1
Psora4	35.37
	35.45
	35.11
SR2640	35.34
	35.29
	34.79
Karanjin	35.74
	34.97
	35.08
6 dpf	
<i>actb</i>	Cq
control	22.91
	22.82
24DB	22.95
	23
GNTI	22.98
	22.81
Psora4	23.13
	22.66
SR2640	22.83
	22.92
Karanjin	23.28
	22.61
<i>ins</i>	
control	29.6
	29.83
GNTI	29.37

	29.5
24DB	29.28
	29.02
Psora4	29.14
	28.92
SR2640	28.62
	28.52
Karanjin	28.46
	28.49
<i>neurod1</i>	
control	32.86
	31.74
24DB	30.35
	30.47
GNTI	30.13
	31.73
Psora4	29.54
	30.3
SR2640	29.11
	29.41
Karanjin	28.75
	29.22
<i>pax6b</i>	
control	29.36
	28.85
24DB	28.53
	2.49
GNTI	30.32
	29.03
Psora4	28.7
	28.55
SR2640	28.79
	28.4
Karanjin	28.23
	28.4
<i>pdx1</i>	
control	35.16
	34.8
24DB	31.96
	30.95
GNTI	31.21
	34.74
Psora4	30.22
	29.97
SR2640	33.1
	30.81

Karanjin	31.85
	32.36
<i>mnx1</i>	
control	33.17
	32.66
24DB	30.83
	31.7
GNTI	31.91
	32.12
Psora4	30.34
	30.95
SR2640	30.66
	29.98
Karanjin	29.81
	30.16
<i>gcga</i>	
control	33.06
	33
24DB	32.8
	32.36
GNTI	32.94
	33
Psora4	33.36
	33.04
SR2640	32.25
	32.22
Karanjin	32.79
	32.23
adult	
<i>actb</i>	Cq
control	26.72
	26.53
24DB	26.88
	26.35
GNTI	26.6
	26.57
Psora4	26.8
	26.47
SR2640	26.78
	26.61
Karanjin	26.65
	26.77
<i>ins</i>	
control	31.4
	31.17

24DB	32.19
	31.75
GNTI	33.45
	33.03
Psora4	26.31
	25.84
SR2640	26.25
	26.1
Karanjin	29.44
	29.43
<i>neurod1</i>	
control	36.95
	35.63
24DB	38.79
	36.58
GNTI	38.57
	37.3
Psora4	33.84
	34.07
SR2640	33.97
	33.61
Karanjin	35.63
	35.4
<i>pax6b</i>	
control	35
	34.68
24DB	35.26
	35.03
GNTI	36.02
	35.53
Psora4	32.82
	32.25
SR2640	32.6
	32.32
Karanjin	34.14
	33.89
<i>pdx1</i>	
control	37.38
	37.59
24DB	36.97
	36.94
GNTI	37.23
	37.79
Psora4	35.48
	35.16
SR2640	35.3

	35.11
Karanjin	35.77
	36.17
<i>mnx1</i>	
control	35.73
	37.04
24DB	36.12
	36.99
GNTI	36.99
	37.56
Psora4	32.8
	32.14
SR2640	33.16
	33.19
Karanjin	34.3
	33.53
<i>gcga</i>	
control	35.6
	35.18
24DB	34.9
	34.41
GNTI	36.69
	35.74
Psora4	30.72
	30.43
SR2640	31.81
	31.83
Karanjin	34.91
	34.6
mouse islets	
<i>Hprt1</i>	Cq
DMSO	25.34
	25.50
	25.24
	25.31
	25.44
	25.91
	25.26
Psora4	25.15
	25.34
	25.68
	25.02
	25.10
	25.66
Pap-1	25.88

	25.13
	25.28
	25.52
	25.41
	25.39
<i>Ins1</i>	
DMSO	15.96
	16.32
	16.11
	16.22
	16.68
	17.13
	17.06
Psora4	15.95
	16.04
	16.64
	16.28
	16.41
	16.61
Pap-1	16.53
	15.92
	16.23
	16.07
	16.33
	16.91
<i>Ins2</i>	
DMSO	13.58
	13.65
	13.53
	13.35
	13.65
	14.32
	14.08
Psora4	13.41
	13.39
	14.01
	13.22
	13.45
	13.65
Pap-1	13.43
	13.07
	13.27
	13.28
	13.33
	13.90